Coastal Engineering 175 (2022) 104140

Contents lists available at ScienceDirect

Coastal Engineering

journal homepage: www.elsevier.com/locate/coastaleng

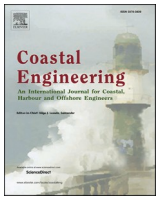

Wave downscaling strategies for practical wave agitation studies in harbours

Eva Romano-Moreno *, Gabriel Diaz-Hernandez, Javier L. Lara, Antonio Tomás, Francisco F. Jaime

IHCantabria - Instituto de Hidráulica Ambiental de la Universidad de Cantabria, Santander, Spain

ARTICLE INFO

Keywords:
Harbour wave agitation
Wave climate
Multimodal wave spectra
Hybrid wave downscaling
Dynamic wave downscaling

ABSTRACT

An accurate estimation of the historical harbour wave agitation is fundamental for many practical applications, such as port downtime analyses. In practical harbour agitation studies, usually based on numerical propagations from offshore wave climate towards a harbour (wave downscaling), the accuracy in defining the outer wave climate has an impact on wave agitation estimations, especially important for multimodal wave climates. In this paper, several strategies for wave agitation downscaling are presented based on different existing approaches with different accuracy levels for: a) wave downscaling method; b) definition of outer spectral waves. The accuracy/performance of each approach is evaluated by applying, and comparing them with multi-point instrumental data from a field campaign, in a real scenario (Africa basin, Las Palmas Port, Spain) where the multimodality of waves, in addition to the agitation effects from port structures in the far-field, clearly determines the final accuracy of the in-port wave agitation. Improved results have been achieved with the most sophisticated/accurate strategies proposed. A comparative analysis of the advantages, limitations, uncertainty and CPU effort of each one, allows to suggest the preferable strategy, in each situation/context, for practical port wave agitation studies.

1. Introduction

An accurate estimation of the historical harbour wave agitation is fundamental for many practical applications, such as port operability/downtime analyses. At present, practical wave agitation studies consist of the characterization of the harbour agitation response, in terms of exceedance thresholds of significant wave height (Hs). They are used to define the operational/downtime/security conditions (ROM3.1-99, del Estado, Puertos, de Fomento, Ministerio, 1999; Thoresen, 2003; PIANC, Working group PTC II-24, 1995).

In common practice, wave agitation response is today accomplished through a numerical modeling approach by transferring defined wave climate conditions from offshore locations to inside the harbour. Therefore, the overall quality of wave agitation characterization greatly depends on: A) the efficiency of the numerical strategy, including numerical model and methodology followed to model the outer-harbour wave propagation and wave penetration into the harbour basin, as well as, B) the accuracy in the definition of forcing wave climate in the vicinity of the harbour.

With respect to the first aspect (A), among the different numerical approaches available in literature, the two most widely used wave agitation models are those based on the elliptic mild-slope or Boussinesq equations. Both model classes solve the main physical processes involved in wave propagation and penetration into the harbour using a 2DH (depth-averaged) approach, providing effective tools to properly simulate and evaluate the harbour wave agitation for practical purposes (Diaz-Hernandez et al., 2021; Eikema et al., 2018; Gruwez et al., 2012). To transfer the historical/hindcast wave conditions from outside to inside the harbour, different approaches can be adopted. On one hand, a dynamic wave downscaling (based on an hour-by-hour numerical modeling) provides the most rigorous method since every historical sea state is numerically propagated. However, this first approach requires a high computational cost incompatible for practical applications. On the other hand, a statistical downscaling approach (completely based on mathematical/statistical techniques) consist of correlating the in-port waves to outer wave conditions by means of mathematical algorithms

* Corresponding author.
E-mail addresses: eva.romano@unican.es (E. Romano-Moreno), gabriel.diaz@unican.es (G. Diaz-Hernandez), jav.lopez@unican.es (J. L. Lara), antonio.tomas@unican.es (A. Tomás), francisco.jaime@unican.es (F. F. Jaime).

https://doi.org/10.1016/j.coastaleng.2022.104140
Received 20 December 2021; Received in revised form 10 March 2022; Accepted 15 April 2022
Available online 26 April 2022

(e.g. increasingly used artificial neural networks, in Kankal and Yüksek, 2012 and López et al., 2015). This approach is limited by the availability of required databases of outer wave conditions and corresponding harbour wave agitation (instrumental data in López et al., 2015, physically modeled in Kankal and Yüksek, 2012). Such databases are usually spatially and/or time limited. Finally, the most commonly used approach is hybrid downscaling. It combines both numerical modeling and statistical/mathematical techniques. Based on a reduced number of numerical propagations, a reference dataset of wave agitation is generated, from which statistical/mathematical techniques are applied to estimate the long-term wave agitation response related to outer waves. Different hybrid methodologies for wave agitation downscaling can be found in literature. For example, in Londhe and Deo (2003) and Zheng et al. (2020), the application of aforementioned neural networks, trained with numerical data, previously generated, is proposed for wave agitation estimation. On other hand, several works are based on the hybrid methodology described in Camus et al. (2013) (originally developed for coastal wave downscaling, demonstrating an efficient performance), applied to port agitation assessment (Campos et al., 2019; Camus et al., 2019; Diaz-Hernandez et al., 2021). According to Camus et al. (2013), a first selection of representative sea states (to be numerically propagated) by applying mathematical selection algorithms is carried out, and a final (statistical) historical reconstruction by means of interpolation methods is performed. This method is applied in a multivariate space.

With respect to the second point (B), the characterization of the wave climate in the vicinity of the harbour is a fundamental aspect, since the wave agitation response is clearly determined by the incoming/forcing waves. In practice, the characterization of the climatic wave conditions outside the harbour is usually based on time series of aggregated wave parameters (typically, significant wave height, Hs; peak period, Tp; and mean direction, Dm) mainly obtained from either hindcast/modeling or instrumental buoy data. Based on this parameterized definition of waves, theoretical spectra (e.g. Jonswap, Pierson Moskowitz) are usually reconstructed and used as input to force numerical agitation models (Gruwez et al., 2012; Panigrahi et al., 2015; Zheng et al., 2020). However, this aggregated information does not represent the multimodal nature of waves usually composed of one or more swells coming from different areas and one wind sea locally generated. This can be a critical point for wave agitation assessment in harbour areas with a clear multimodality of waves. Each particular wave system, with different period and/or direction, penetrates into the harbour basin influencing, in a different manner, the wave agitation response. Aggregated unimodal definitions for outer waves in sea states comprised by multiple waves, result in deviated agitation patterns. For more accurate estimations of wave agitation response, with multimodal outer waves, multi-peaked spectral representations forcing the numerical agitation model are required. In the last years, new spectral-based approaches, relying on directional spectral information, for multimodal wave climate definition have been developed. For example, Rueda et al. (2017) is based on long-term time series of (9-variable) sets of parameters (Hs_i, Tp_i, Dm_i; where $i = 1$ to 3) to describe three wave systems (parameterized partitions from directional spectra) in each sea state. From time series like this, for each sea state, the partitioned spectrum of each parameterized component can be theoretically reconstructed to ultimately compose the (total) multi-peaked spectrum as a superposition of the corresponding partitions. This reconstructed spectra provides an approximated spectral representation of multimodal waves. Nevertheless, the most accurate way to represent the spectral wave climate is by means of the real-shaped spectra. Nowadays, the complete directional spectrum of a sea state in a specific location can be numerically obtained. This is possible due to the advances of the third generation spectral wave models that allow to resolve the complete directional energy distribution of waves during the propagation processes in offshore and nearshore. This latter, in addition to the advances of reanalysis data used as forcing of these models results in improved hindcast/modeling of directional spectra (Perez et al., 2017). Wave climate definition based on the complete directional spectra acquires special importance as forcing for numerical agitation models since they provide detailed representations of the multimodal outer waves. By means of numerical agitation models able to assimilate and propagate the real-shaped directional spectra, more accurate numerical wave agitation results can be estimated. Indeed, this can be considered as one of the new advances in the state of art of numerical wave agitation modeling (Diaz-Hernandez et al., 2021).

The objective of this work is to assess the performance of different approaches for historical wave agitation characterization, measuring the associated uncertainty level and computational cost. A two-stage wave downscaling procedure is proposed, comprising the following stages: 1) a dynamic wave downscaling, from offshore to near-port; 2) wave downscaling from outer waves to port agitation. An accurate real-shaped (not parameterized/theoretical functions) definition of spectral wave climate in the vicinity of the port (hindcast series) has been achieved in the first stage of a dynamic wave downscaling. In the second stage of wave downscaling, six different strategies for wave propagation and wave penetration into the harbour basin have been developed. First, a wave agitation downscaling following a dynamic approach is presented. The other 5 strategies proposed consist of different adaptations/versions of hybrid downscaling, based on the aforementioned general methodology described in Camus et al. (2013), depending on the different sub-approaches (accuracy levels) adopted to define the multi-annual outer spectral wave climate (theoretical based on unimodal aggregated parameters, trimodal parameterized partitions, or multimodal real-shaped) at each step of the methodology. All the strategies have been applied to a real port area (Africa basin, Las Palmas Port, Spain) with a clearly multimodal wave climate, where, in addition, the far-field agitation effects generate characteristic (in principle not expected) local agitation patterns. The uncertainty is progressively quantified, from the initial value associated with the offshore input data and throughout the entire downscaling procedure for each different strategy, by comparing the numerical data with on-site measurements. The performance of each different strategy is quantitatively evaluated in terms of accuracy and computational cost. The advantages and limitations for each one are pointed out allowing to suggest the best strategy to follow for practical wave agitation studies depending on the context, where the main conditioning factor is the available initial information database describing the historical wave climate offshore/outside the port.

This paper is organized as follows: Section 2 briefly describes the study port basin where the different proposed strategies are applied, as well as the instrumental data used in validating each stage of the entire downscaling process, for each different strategy. In section 3, the dynamic procedure followed to generate the hindcast series of real-shaped spectra outside the port is firstly described. Then, a characterization of the historical spectral wave climate in the vicinity of the port is presented. In section 4, the different downscaling strategies for wave agitation are described, including a final analysis of the different approaches adopted to define the forcing spectra of wave agitation model and their effects on numerical results. Section 5 presents the results obtained with each strategy, evaluating and discussing the performance of each one. Finally, section 6 contains the main conclusions of this work.

2. Study port basin and instrumental data used for validation

The Africa basin (Fig. 1a) is located in Las Palmas Port, which is on the East coast of Gran Canaria Island, open to Atlantic Ocean (Fig. 2). It has a north-south orientation with the port entrance on the southern side. The main protection structure is the Nelson Mandela breakwater (vertical breakwater made of concrete caissons; 1 000 m long, approximately) that bounds the eastern boundary of the basin. On the west side, the basin is delimited by the Reina Sofia breakwater. It consists of a rubble mound breakwater in the north-south aligned section (1 600 m

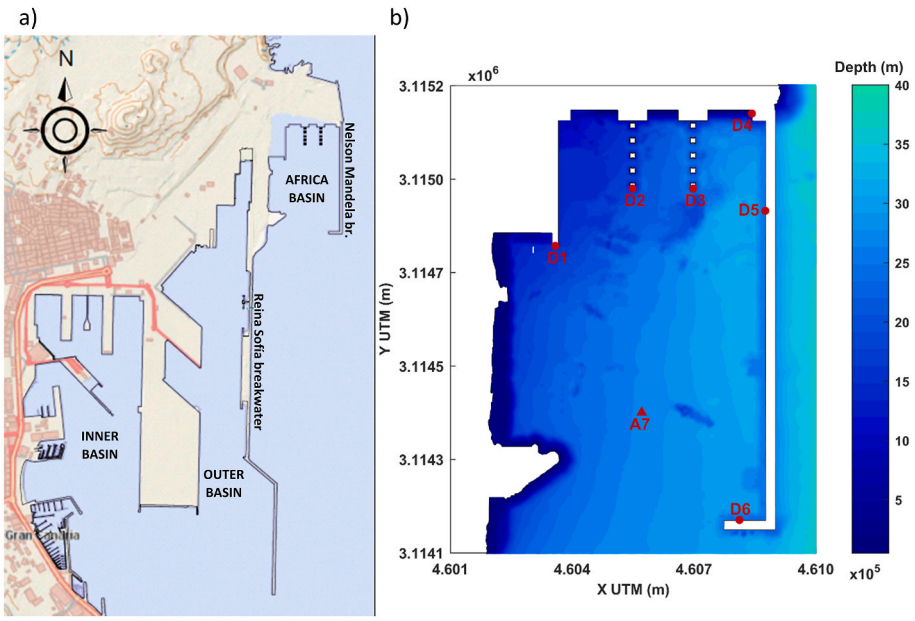

Fig. 1. a) Location of the Africa basin in Las Palmas Port. Actual port geometry. Source of base map: viewfinder Grafcan (IDE Canarias, Government of the Canary Islands). b) Location of measuring systems in the Africa basin (DeepWAVES: D1-D6, AWAC: A7). UTM coordinates (m). Actual bathymetry (m).

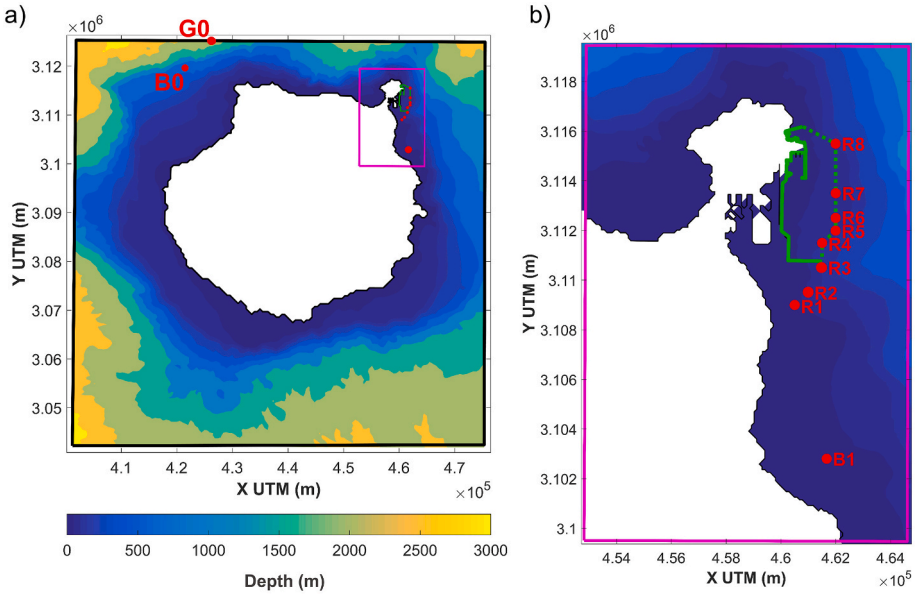

Fig. 2. a) Numerical grids defined in SWAN. Low resolution (black): dx = dy = 0.005º; Fine resolution (magenta): dx = dy = 0.001º. Position of control points B0 and G0. Numerical domain in MSP (green). b) Numerical domain in MSP within the fine grid in SWAN. Position of control point B1 and forcing points in MSP (R1–R8). UTM coordinates. Actual bathymetry (m).

long, approximately), and vertical wall in its final part (1 400 m long, approximately). Inner contours, on the north and east sides, are mainly built of vertical type quay walls (concrete caissons), and rubble mound cross-sections between berthing ramps in the northern contour. The western side of the basin (unfinished construction) consist of natural slope and fill. The water depth in the basin varies up to nearly 35 m (at high water level, Fig. 1b).

The instrumental data used to validate the proposed wave downscaling procedures come from three different sources depending on the phase of the methodology to be validated. First, offshore waves (used as initial forcing in wave downscaling) have been validated prior to start the downscaling process. This validation is based on a comparison with instrumental data from an offshore buoy (Gran Canaria buoy, REDEXT, provided by the Spanish institution Puertos del Estado) located in the north of Gran Canaria island at deep waters (UTM coordinates: 421486.27 m E, 3119616.75 m N; 780 m depth; B0 in in Fig. 2a). It is a SeaWatch buoy (since 2003) with a recording time period of 30 min every hour (del Estado, Puertos, de Fomento, Ministerio, 2015a). Hourly scalar aggregated parameters are provided for a length of over 22 years (1997–2019) as well as directional aggregated parameters are available for a period of 16 years (2003–2019).

The outer waves in the vicinity of the port, numerically obtained in the first stage of downscaling, have been validated with data from a coastal buoy (Las Palmas Este buoy, REDCOS, provided by Puertos del Estado) located in the proximities of the port (UTM coordinates: 461671.76 m E, 3102802.49 m N; 30 m depth; B1 in Fig. 2b). It is a

Triaxys buoy (since 2014) with a recording time period of 24 min every hour, with a sampling rate of 4 Hz (del Estado, Puertos, de Fomento, Ministerio, 2015b). Hourly scalar aggregated parameters are provided for a length of 28 years (1992–2020) as well as directional aggregated parameters are available for a period of 6 years (2014–2020).

Instrumental data for multi-position validation of wave agitation inside the port (second stage of wave downscaling procedure) consist of data measured in a field campaign performed in the Africa basin from July 2019 to February 2020 (8 months). Wave agitation measurements were taken at different locations along the berthing line by means of DeepWAVES monitoring stations. Free surface measurements are taken by means of ultrasonic range finders, with a sample rate of 5 Hz. For a period of one month (July 2019), an Acoustic Wave and Current Profiler with Acoustic Surface Tracking (AWAC-AST, Nortek AS) was deployed in the middle of the Africa basin. This instrument used a pressure and velocity sampling rate of 2 Hz (that is 4 Hz for surface tracking, (Nortek, 2017)). Hourly wave parameters are obtained from postprocessing the measured data from DeepWAVES and AWAC systems for the same 20 min every hour. Fig. 1b shows the location of the gauges employed in this validation process (DeepWAVES: D1-D6 and AWAC: A7).

3. Historical spectral wave climate in the vicinity of the port

A proper multi-annual outer spectral wave climate definition in the vicinity of the port has been attained by means of historical time series of real-shaped (not parameterized or theoretical functions) directional spectra, so that the multimodal nature of waves is conserved and completely represented when forcing the wave agitation model. This point is especially relevant for wave agitation studies where the modality of the outer waves plays an important role in the response of the basin. Historical series of over 40 years (1980–2020) with hourly directional wave energy spectra have been generated in the proximities of the port basin by means of the third-generation spectral wave model SWAN (Simulation Waves Nearshore; (Booij et al., 1999)) used in a dynamic/non-stationary mode. Two nested grids (Fig. 2a) have been defined, reaching a resolution of 0.001° in the port area (fine mesh). Hourly forcings come from global hindcast and reanalysis data: wind fields (10 m height) from the Climate Forecast System (CFSR) (Saha et al., 2010), (CFSv2) (Saha et al., 2014); wave contours (offshore directional spectra with spatial resolution of 0.25°) from the Global Ocean Waves (GOW2) database (Perez et al., 2017); sea level including

Table 1
Summary table of numerical strategies. Characteristics of wave definition approaches at each step from S1 to S6. The accuracy in representing the multimodality of waves is indicated by the color scale (in descending order: green, yellow, orange, and red). Wave parameters: Hm_0; Tp; Dm; directional spreading, σ_D; peak enhancement factor, γ Jonswap. LWL: Low Water Level; HWL: High Water Level.

STRATEGY	**S1. DYNAMIC, REAL-SHAPED**	**S2. HYBRID, STANDARD THEORETICAL UNIMODAL**	**S3. HYBRID, CHARACTERISTIC THEORETICAL UNIMODAL**	**S4. HYBRID, COMBINED**	**S5. HYBRID, CHARACTERISTIC THEORETICAL MULTIMODAL**	**S6. HYBRID, REAL-SHAPED**
Downscaling	Dynamic	Hybrid	Hybrid	Hybrid	Hybrid	Hybrid
Historical outer wave climate definition **(Hindcast series)**	**Real-shaped** spectra	Sets of **3 aggregated parameters** (Hm_0, Tp, Dm)	Sets of **5 aggregated parameters** (Hm_0, Tp, Dm, σ_D, γ)	Sets of **3 aggregated parameters**[1] (Hm_0, Tp, Dm)	**3 parameterized partitions.** 3 sets of 5 aggregated parameters 3x (Hm_0, Tp, Dm, σ_D, γ)	**Real-shaped** spectra
Selection representative cases (MaxDiss)	-	Sets of **3 aggregated parameters** (Hm_0, Tp, Dm)	Sets of **5 aggregated parameters** (Hm_0, Tp, Dm, σ_D, γ)	Sets of **3 aggregated parameters** (Hm_0, Tp, Dm)	**3 parameterized partitions.** 3 sets of 5 aggregated parameters 3x (Hm_0, Tp, Dm, σ_D, γ)	**Real-shaped** spectra
Forcing spectra definition	**Real-shaped**	**Standard theoretical unimodal**	**Aggregated theoretical unimodal**	**Real-shaped**	**Partitioned theoretical multimodal**	**Real-shaped**
Sea level definition	**Real** values	Linear **interpolation** (LWL and HWL)	Linear **interpolation** (LWL and HWL)	Linear **interpolation** (LWL and HWL)	Linear **interpolation** (LWL and HWL)	Linear **interpolation** (LWL and HWL)
Wave agitation **propagations**	**Hourly historical** sea states	**Selected** sea states	**Selected** sea states	**Selected** sea states	**Selected** sea states	**Selected** sea states
Historical reconstruction (RBF interpolation)	-	Sets of **3 aggregated parameters** (Hm_0, Tp, Dm)	Sets of **5 aggregated parameters** (Hm_0, Tp, Dm, σ_D, γ)	Sets of **3 aggregated parameters** (Hm_0, Tp, Dm)	**3 parameterized partitions.** 3 sets of 5 aggregated parameters 3x (Hm_0, Tp, Dm, σ_D, γ)	**Real-shaped** spectra

[1]Real-shaped spectra for the reduced number of the selected representative sea states are required.

astronomical tide and storm surge from Global Ocean Tide (GOT) (IHCantabria reconstruction based on the TPXO global tides model (Egbert et al., 1994; Egbert and Erofeeva, 2002)) and Global Ocean Surges (GOS) (Cid et al., 2014) datasets, respectively.

In order to perform a robust wave validation throughout the entire procedure, quantifying the uncertainty introduced at each phase of downscaling, the historical offshore waves from GOW database used as forcing in SWAN model (at point G0 in Fig. 2a) have been compared with instrumental data from an offshore buoy (780 m deep; B0 in Fig. 2a). Variations between these two close positions at deep waters are considered to be negligible. Indeed, high correlated results are obtained comparing wave characteristics at both locations. Additionally, numerical results from SWAN at point B0 have also been compared with instrumental data. The quality of the numerical offshore waves has been quantitatively evaluated by means of the main statistical parameters (systematic deviation, BIAS; root mean square error, RMSE; dispersion from bisector as Scatter Index, SI; bisector correlation coefficient, CORR; and the correlation ratio, R^2) in Table 3. High goodness in the fitting is shown at both positions G0 and B0. For zero order moment wave height (Hm_0 parameter), RMSE of 0.25 m and SI of 0.15 are obtained, while CORR and R^2 are above 0.92 and 0.85, respectively (Table 3). An adequate representation of offshore waves is demonstrated, as well as the initial uncertainty level associated with the input data at the first stage of wave downscaling is quantified.

From numerical model SWAN, long time series of outer wave spectra (discretized in 41 frequencies x 48 directions) have been obtained at 9 different positions in the vicinity of the port (B1; R1-R8 in Fig. 2b). Control point B1 (about 30 m deep) has been used to validate these numerical propagations (first stage in dynamic methodology). Time series at points R1-R8 (about 100 m deep) have been generated in order to represent the spatial variability over the area when forcing the wave agitation model.

The directional spectral waves dynamically simulated at point B1 are compared with those obtained from instrumental data of the coastal buoy. Comparison (scatter plots and main statistical/correlation parameters) between buoy and numerical aggregated spectral parameters are shown in Fig. 3. The assessment coefficients are also indicated in Table 3. An adequate goodness of fit of numerical estimations, in terms of spectral parameters, is shown at the coastal analysis position B1. CORR coefficients of 0.91, 071 and 0.80 are obtained for comparisons of Hm_0, Tm_{02} and Tp, respectively. CORR = 0.75 is obtained for both directional parameters Dm and Dp. Some deviation is observed in scatter plot of Dm parameter, where some values of aggregated Dm from numerical modeling are considerably different from instrumental Dm values from the buoy (e.g., $Dm_{MODEL} > 145°$ for $Dm_{BUOY} < 145°$). It should be noted that those deviated data represent a 0.28% of the total length of 6 years of wave statistics used in comparison. Such deviations are due to local wind effects. Since meso-scale resolution wind fields have been used to force the SWAN model, possible local "shadow" effects from the local topography of the island are not well represented when winds come from onshore. This results in an overestimation of such locally-generated sea waves coming from NW directions. Nevertheless, the in-port wave agitation is not affected by these waves since their propagation direction is opposite to that incident to the port, so these deviations are not considered to affect the goodness of fit of validation.

After this validation at the coastal position B1, the directional spectra at points R1-R8 are used to characterize the historical spectral wave climate in the vicinity of the port. This information is later used to define the forcing wave climate for the wave agitation model, by following the

Table 2
Results of Hm_0, Tp and Tm_{02} at 7 control points by forcing the wave agitation modeling with spectra a) – e) (Fig. 8).

		Real-shaped			Standard, theoretical, unimodal 3 parameters: Hm_0, Tp, Dm			Characteristic, theoretical, unimodal 5 parameters: Hm_0, Tp, Dm, σ_D, γ			Characteristic, theoretical, multimodal 3x5 parameters: 3x(Hm_0, Tp, Dm, σ_D, γ)		
		Hm_0 (m)	Tp (s)	Tm_{02} (s)	Hm_0 (m)	Tp (s)	Tm_{02} (s)	Hm_0 (m)	Tp (s)	Tm_{02} (s)	Hm_0 (m)	Tp (s)	Tm_{02} (s)
a)	**D1**	0.23	5.7	5.3	0.17	9.9	9.9	0.18	10.6	10.0	0.18	10.6	10.0
	D2	0.24	4.7	5.0	0.16	10.0	9.7	0.18	10.0	9.7	0.18	10.0	9.7
	D3	0.20	5.5	5.5	0.15	9.2	9.5	0.16	9.6	9.4	0.16	9.6	9.4
	D4	0.18	6.5	5.4	0.15	11.2	10.5	0.16	11.2	10.5	0.16	11.2	10.5
	D5	0.20	5.4	5.2	0.16	10.1	9.8	0.17	10.5	9.7	0.17	10.5	9.7
	D6	0.18	9.1	6.5	0.17	9.1	9.6	0.17	9.2	9.7	0.17	9.2	9.7
	A7	0.21	5.8	5.6	0.16	10.6	10.1	0.17	11.7	10.2	0.17	11.7	10.2
b)	**D1**	0.17	10.0	7.4	0.11	9.5	9.4	0.13	9.9	9.2	0.11	3.0	3.4
	D2	0.15	11.8	7.3	0.10	10.9	9.4	0.14	10.4	8.8	0.12	3.0	3.3
	D3	0.14	11.0	8.7	0.11	9.1	9.2	0.14	9.1	8.3	0.10	3.0	3.5
	D4	0.14	12.0	9.7	0.10	11.1	10.3	0.12	11.0	9.1	0.11	3.0	3.4
	D5	0.14	12.0	7.8	0.10	9.9	9.4	0.13	10.3	8.4	0.11	3.3	3.5
	D6	0.15	10.2	9.2	0.12	9.1	9.5	0.13	9.8	9.1	0.10	3.7	4.0
	A7	0.16	10.8	8.5	0.11	9.2	9.5	0.13	10.6	8.9	0.10	3.0	3.5
c)	**D1**	0.70	4.2	4.3	0.32	12.2	12.0	0.31	12.5	11.7	1.05	4.3	4.2
	D2	0.28	3.5	4.7	0.34	12.1	11.4	0.31	12.1	10.8	0.34	3.6	3.9
	D3	0.21	7.6	6.3	0.28	12.1	11.1	0.27	12.2	10.7	0.21	4.8	4.8
	D4	0.21	15.0	8.4	0.29	12.6	12.0	0.28	13.8	12.2	0.18	5.3	6.0
	D5	0.20	12.3	7.0	0.29	12.1	11.3	0.26	12.1	11.2	0.19	4.3	5.2
	D6	0.23	5.1	5.7	0.24	12.1	11.3	0.25	12.0	10.9	0.26	5.1	4.7
	A7	0.38	3.9	4.5	0.36	12.3	12.2	0.34	13.2	11.9	0.49	4.0	4.1
d)	**D1**	0.81	4.1	4.2	0.56	9.1	8.5	0.49	9.8	8.3	0.49	4.7	4.4
	D2	0.51	4.2	4.4	0.68	9.4	7.6	0.59	9.9	7.4	0.37	4.6	4.6
	D3	0.37	5.2	4.9	0.71	8.7	7.8	0.54	8.6	7.5	0.28	5.4	5.0
	D4	0.34	5.2	5.3	0.42	8.6	7.3	0.38	9.5	7.3	0.27	8.3	5.8
	D5	0.36	4.7	4.8	0.54	8.4	7.4	0.45	7.7	7.2	0.28	5.4	5.1
	D6	0.32	4.9	4.9	0.50	9.3	8.1	0.47	9.9	8.2	0.29	5.2	5.2
	A7	0.51	4.1	4.5	0.60	8.8	7.9	0.51	8.1	7.8	0.38	5.2	5.1
e)	**D1**	0.42	4.5	4.6	0.21	4.7	4.6	0.25	4.7	4.5	0.36	4.7	4.5
	D2	0.34	4.3	4.6	0.29	4.7	4.6	0.39	4.5	4.6	0.29	4.6	4.6
	D3	0.29	5.2	5.2	0.33	5.1	5.0	0.35	5.3	5.0	0.27	5.2	5.2
	D4	0.29	6.1	5.7	0.30	5.2	4.9	0.31	5.4	4.7	0.28	7.8	5.8
	D5	0.29	5.0	5.0	0.30	5.0	4.7	0.34	5.2	4.7	0.27	5.2	5.1
	D6	0.24	5.1	5.4	0.20	5.3	4.9	0.24	5.1	4.8	0.22	5.6	5.5
	A7	0.32	4.9	4.9	0.26	5.0	4.8	0.30	4.9	4.7	0.29	5.1	5.0

Table 3
Statistical fit coefficients from comparison of numerical data with instrumental measurements at each stage of wave downscaling methodology. Visualization of the uncertainty/accuracy level at each stage throughout the entire downscaling methodology (for different strategies in the second stage of wave agitation downscaling).

	Stage of wave downscaling	Par.	BIAS	RMSE	SI	CORR	R^2	Statistics Length
0.1	**Offshore waves** (Forcing point G0 in SWAN)	Hm_0	−0.062 m	0.250 m	0.150	0.925	0.855	Scalar: 22 years
		Tm	0.168 s	0.996 s	0.182	0.742	0.550	Directional: 16
		Tp	1.220 s	2.670 s	0.288	0.725	0.525	years
		Dm	−11.832°	21.257°	0.111	0.815	0.665	
		σ_D	1.308°	11.916°	0.331	0.693	0.480	
0.2	**Offshore waves** (Results from SWAN at offshore point B0)	Hm_0	0.034 m	0.252 m	0.151	0.924	0.853	Scalar: 22 years
		Tm	−0.042 s	0.983 s	0.179	0.743	0.552	Directional: 16
		Tp	1.403 s	2.663 s	0.287	0.736	0.541	years
		Dm	−12.089°	20.139°	0.105	0.830	0.690	
		σ_D	1.838°	13.080°	0.363	0.661	0.437	
1	**Outer waves in the vicinity of the port basin** (Results from SWAN at coastal point B1)	Hm_0	0.061 m	0.241 m	0.206	0.906	0.822	Scalar: 28 years
		Tm	−0.528 s	1.028 s	0.208	0.707	0.500	Directional: 6 years
		Tp	0.253 s	1.871 s	0.232	0.796	0.634	
		Dm	−8.017°	13.992°	0.350	0.751	0.564	
		σ_D	0.646°	8.336°	0.325	0.642	0.412	
2.1	**S1. Wave agitation inside the port basin** (Results from S1 at inner points D1-D6, A7)	Hm_0	−0.003 m	0.079 m	0.244	0.823	0.677	D1-D6: 8 months
		Tp	−1.186 s	3.001 s	0.385	0.771	0.595	A7: 1 month
2.2	**S2. Wave agitation inside the port basin** (Results from S2 at inner points D1-D6, A7)	Hm_0	−0.088 m	0.137 m	0.422	0.726	0.527	D1-D6: 8 months
		Tp	1.591 s	3.485 s	0.447	0.736	0.542	A7: 1 month
2.3	**S3. Wave agitation inside the port basin** (Results from S3 at inner points D1-D6, A7)	Hm_0	−0.059 m	0.105 m	0.324	0.775	0.601	D1-D6: 8 months
		Tp	1.812 s	3.620 s	0.465	0.732	0.535	A7: 1 month
2.4	**S4. Wave agitation inside the port basin** (Results from S4 at inner points D1-D6, A7)	Hm_0	−0.009 m	0.087 m	0.269	0.797	0.635	D1-D6: 8 months
		Tp	−1.270 s	3.268 s	0.420	0.746	0.557	A7: 1 month
2.5	**S5. Wave agitation inside the port basin** (Results from S5 at inner points D1-D6, A7)	Hm_0	−0.023 m	0.092 m	0.285	0.784	0.615	D1-D6: 8 months
		Tp	0.798 s	3.157 s	0.405	0.745	0.556	A7: 1 month
2.6	**S6. Wave agitation inside the port basin** (Results from S6 at inner points D1-D6, A7)	Hm_0	0.006 m	0.081 m	0.250	0.817	0.667	D1-D6: 8 months
		Tp	0.063 s	3.106 s	0.399	0.742	0.551	A7: 1 month

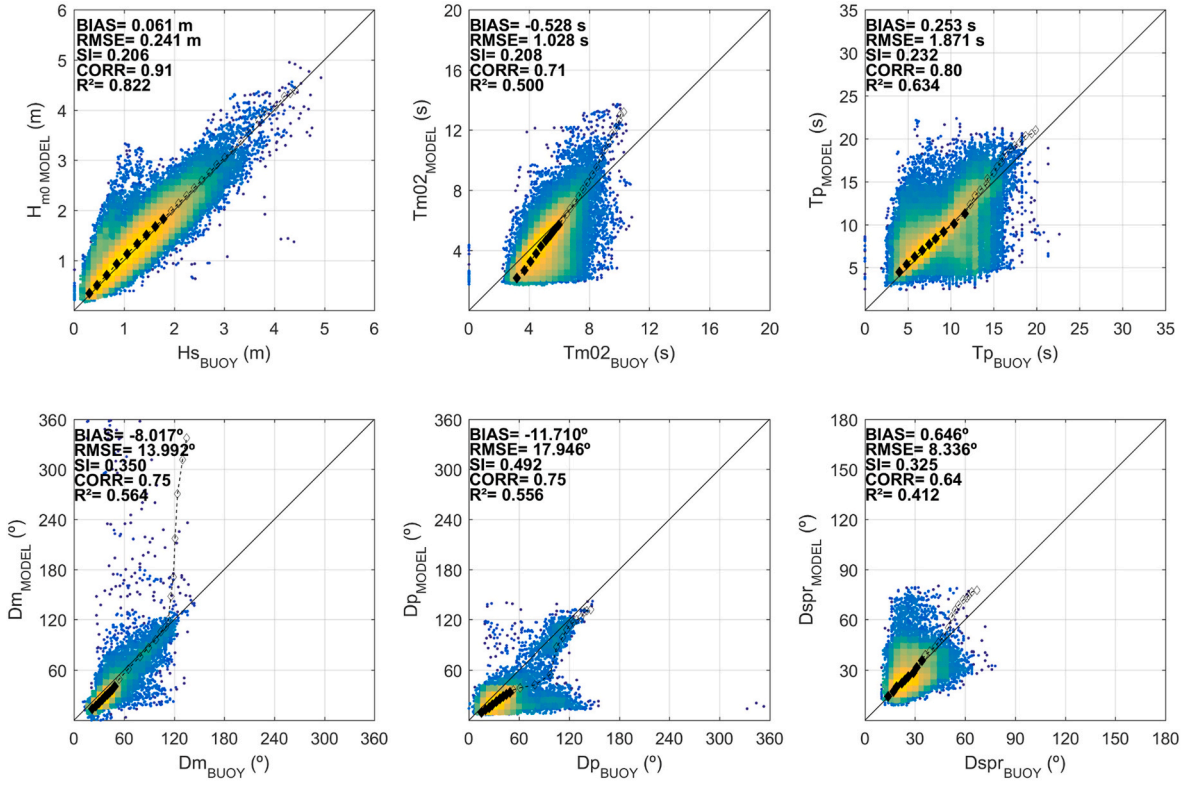

Fig. 3. Scatter plots (and main statistical/correlation coefficients) of aggregated parameters (numerical versus buoy) at control point B1. 28 years of wave statistics for scalar parameters; 6 years of wave statistics for directional parameters. Quantile values for 30 non-exceedance probability values equi-spaced between 1% and 99.999%, in Gumbel probability paper (-ln(-ln(F)); where F is the non-exceedance probability), are represented by diamond symbols (filled color for values between 1% and 90%; non-filled color for values between 90% and 99.999%).

different definition approaches adopted in the different wave downscaling strategies.

The historical spectral wave climate in the vicinity of the study port area presents a strong multimodality of waves. In this historical outer wave climate characterization, the directional spectra have been partitioned making use of the library code Wavespectra (GitHub – metocean/wavespectra, MetOcean Solutions Ltd., 2018) based on the watershed algorithm (Hanson et al., 2009). The statistical analysis of time series of parameterized partitions demonstrates the predominance of multimodal sea states in the study area. For example, 18.4% of the hourly sea states in the historical series at point R6 present a unimodal spectral shape; 27.4% are bimodal cases; 26.7% of spectra present a trimodal shape. The remaining 27.5% correspond to multi-peaked cases (19.3% and 8.2% of spectra with 4 and 5 components, respectively). In Fig. 4, each separate wave component obtained from partitioning each historical directional spectra is represented in a parameterized form. Hm_0 values of different hourly partitioned wave components are illustrated by color scales in a Tp-Dm space. As can be seen in Fig. 4, main wave components predominantly comes from NNE directions with peak periods between 5 and 10 s. Indeed, all unimodal cases in historical time series (with significant wave heights up to 5.7 m) are registered in N-NE directional sectors, with peak period values from 4 to 20 s, mostly contained in the range between 7.5 and 10 s. As the multimodality of waves accentuates, wave heights decrease as well as the variability of partitioned peak periods and wave directions increases. For non-primary wave systems, predominant peak periods, in general, are within 10 and 15 s. In a directional analysis, the aforementioned range (10–15 s) presents the higher probability of occurrence for N-E wave directions; while for E-S directions, the most probable waves come from SE with peak periods between 5 and 7.5 s.

4. Downscaling strategies

Six different strategies for wave agitation downscaling (second stage in a complete wave downscaling procedure) are presented and analyzed in this section. First, a dynamic wave agitation downscaling is developed and validated. Then, five different adaptations/approaches of hybrid downscaling based on the general methodology described in Camus et al. (2013) and Diaz-Hernandez et al. (2021) are presented. The general hybrid methodology is divided in three main steps: i) selection of a reduced number of sea states representative of the historical outer wave climate, by means of the Maximum Dissimilarity (MaxDiss) selection algorithm (Camus et al., 2011b); ii) numerical propagation of representative sea states by using a wave agitation model; iii) statistical reconstruction of the entire historical series of wave agitation by means of Radial Basis Function (RBF) interpolation (Camus et al., 2011a) based on numerical results from ii) and the historical outer wave climate. In this work, the different hybrid methodologies are proposed mainly depending on the approach adopted to define the outer wave spectra at each step of the methodology.

The six practical downscaling strategies proposed in this paper for port agitation assessment are summarized in Table 1.The approach for wave definition at each step of each strategy is indicated, as well as the accuracy in representing the multimodality of the waves is depicted by a color scale. Green color indicates the highest accuracy level, followed by yellow, orange and, finally, red color which indicates the poorest

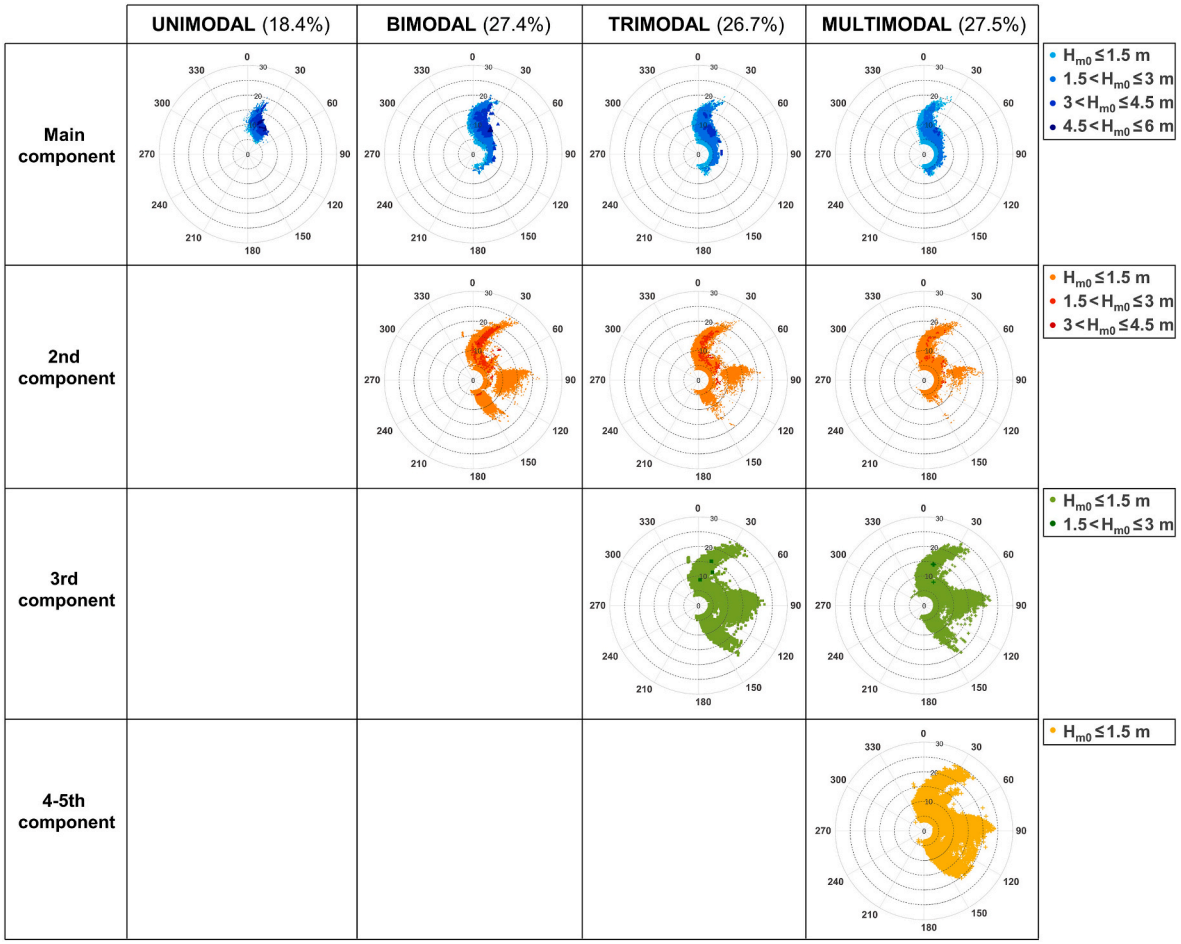

Fig. 4. Wave parameters (Hm_0, Tp, Dm) of separate wave systems in partitioned hourly historical spectra at point R6. Wave heights represented by different color scales in a Period-Direction space, in polar plots. Probability of occurrence (%) of each modality in historical time series.

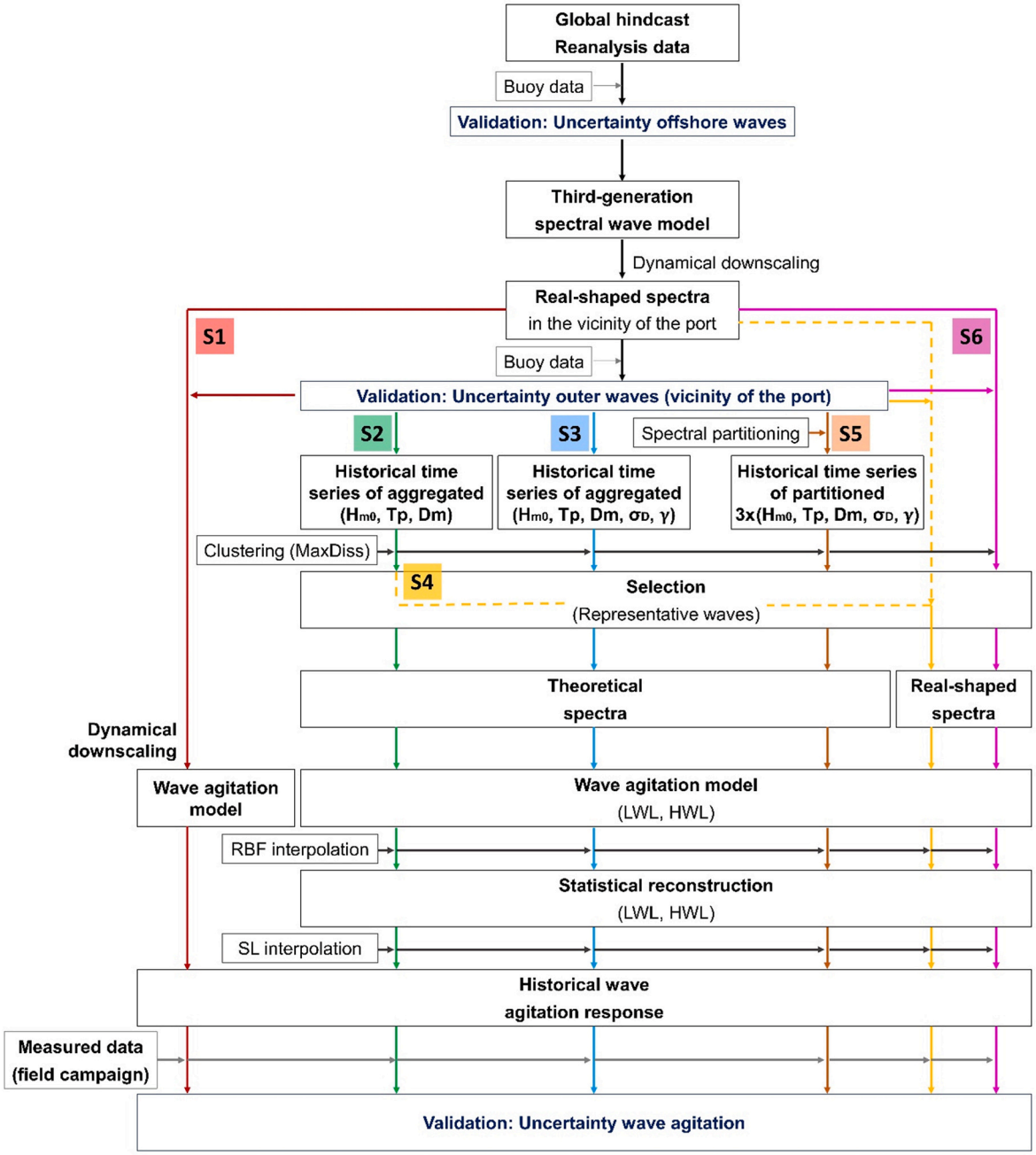

Fig. 5. General scheme of numerical strategies. S1: dynamic downscaling. S2–S6: hybrid downscaling.

representation of multimodal sea states.

Fig. 5 presents the general scheme followed in this work for the dynamic (S1) and hybrid (S2–S6) methodologies. The detailed description of each one is exposed in the following subsections. First, the dynamic strategy is described. Then, the different hybrid methodologies are presented from lower to higher sophistication level.

4.1. S1: Dynamic, real-shaped

In this dynamic approach, the long time series of spectral wave agitation response are numerically simulated in an hourly and continuous way. The procedure followed to transfer the waves inside the port is based on Diaz-Hernandez et al. (2021). The numerical model used in this study is the modified elliptic mild-slope model MSPv2.0 (Diaz-Hernandez et al., 2021) whose improved performance of meshing generator and numerical solver allow high-resolution propagations for short waves over large areas with complex bathymetries and geometries. This is an important aspect in large port areas such as the current study where the collateral far-field agitation effects (inner wave agitation produced by far structures/elements from the basin) plays an important role in wave agitation inside the basin (Sections 4.7 and 5). Another advantage to note is the capacity to self-adapt the numerical reflection coefficient (Kr) of port contours according to the periods of incoming waves (T). In MSPv2.0, the Kr for each contour/structure can be defined varying as a function of T. For example, based on Vílchez et al. (2016) the expressions of Kr(T) curves for some classified coastal/port structure types can be defined according to the typology, geometrical parameters of cross-section, material and water depth. The actual port geometry (2.0 km wide x 5.4 km high, Fig. 2) with 20 different types of cross-section and their associated Kr(T) curves, as well as the detailed

bathymetry (Fig. 2) of the port area have been considered in this work. In addition, the procedure allows to consider the detailed directional wave energy spectra outside the port as forcing in wave agitation modeling, which is an important aspect in multimodal wave climates. The evaluation of the spectral wave agitation is conducted through a spectral reconstruction based on the superposition of energy-denormalized unitary monochromatic waves covering the outer spectral waves (Diaz-Hernandez et al., 2021). This approach provides an efficient computational way to evaluate the wave characteristics at any point inside the port from an incoming directional spectrum (Diaz-Hernandez et al., 2015). It is important to note the validity of this monochromatic-based approach as long as linearity of waves is maintained. Non-linear effects of wave transformation are not simulated. The high computational effort involved in dynamic wave propagations over large numerical domains result excessive with other numerical approaches. This monochromatic-based approach, using a mild-slope agitation model, provides an efficient modeling performance for long-term wave agitation predictions such as those required in the dynamic downscaling method adopted in this strategy. The monochromatic catalogue has been defined for a spectral discretization of 36 frequencies and 72 directions. The wave agitation modeling (propagations with MSPv2.0 and subsequent spectral reconstruction) has been dynamically forced with the hourly spectral information previously generated at points R1-R8 (Fig. 2) and considering the hourly real sea level.

Fig. 6 shows the comparison of wave agitation numerically obtained at each of the control points (Fig. 1b) with that from instrumental data, during the time length of the field campaign (8 months for points D1 to D6, 1 month for point A7). The scatter plots and their main statistical and correlation parameters are presented in Fig. 6. Adequate correlation values (CORR $\geq$ 0.82 and $R^2 \geq 0.67$) between measured and numerical data have been obtained for all the control points except for the point D1 where the coefficients are lower (CORR = 0.72, $R^2 = 0.52$). The low BIAS values also indicate the good approximation between the numerical reconstruction and measurements.

The good performance of the numerical assembly has been also

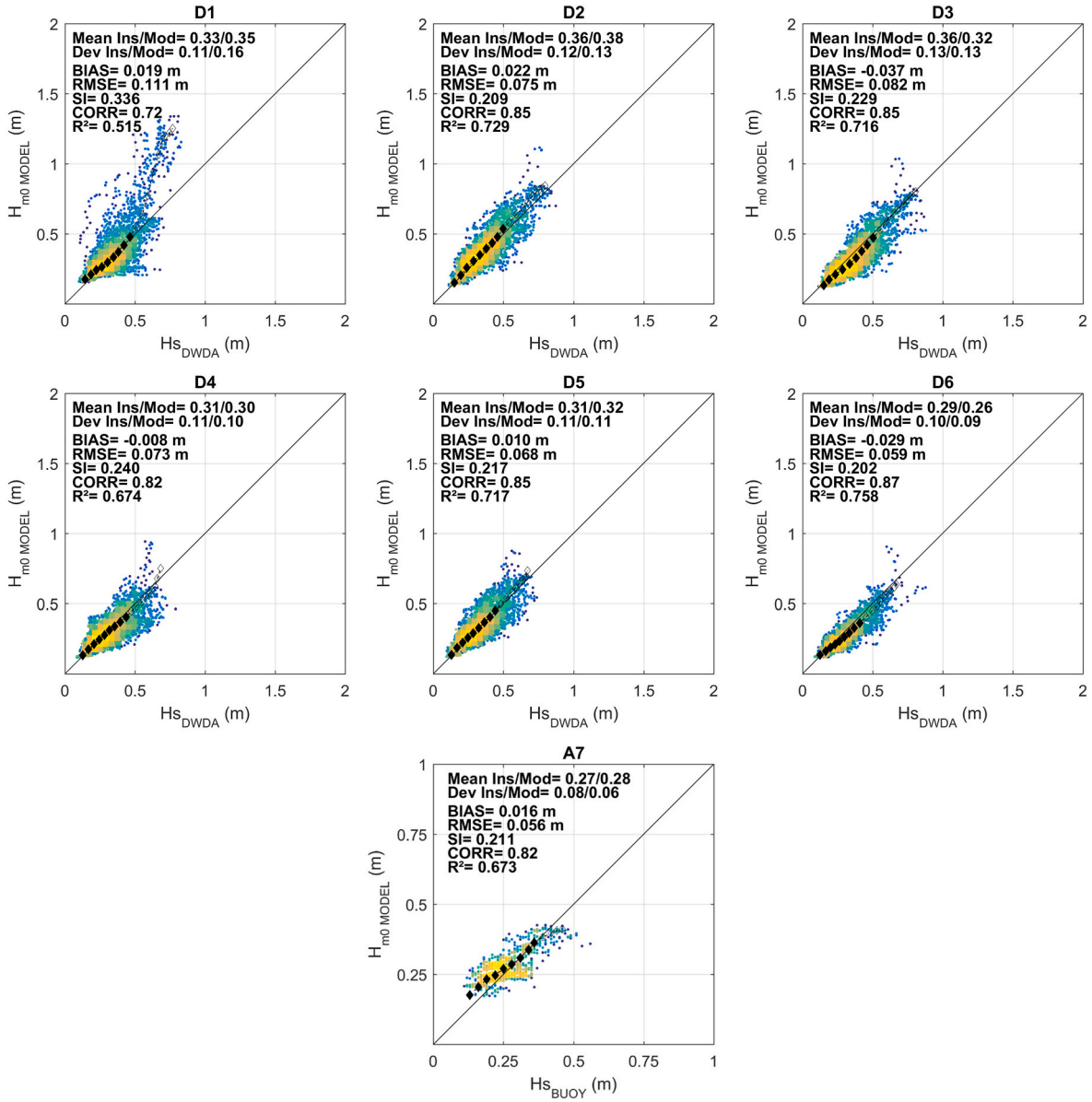

Fig. 6. Scatter plots of wave agitation (numerical results versus field data) at the control points D1-D6 (DeepWAVES) and point A7 (AWAC). Quantile values for 30 non-exceedance probability values equi-spaced between 1% and 99.999%, in Gumbel probability paper, are represented by diamond symbols (filled color for values between 1% and 90%; non-filled color for values between 90% and 99.999%).

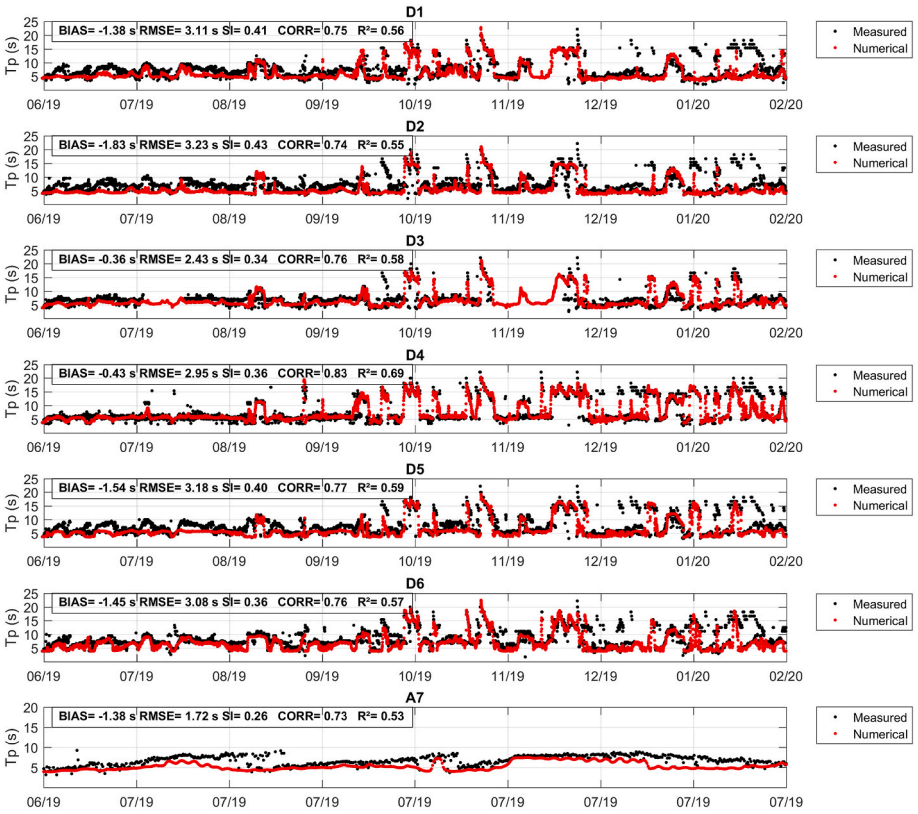

Fig. 7. Time series of Tp (s) at the control points D1-D6 (DeepWAVES, 8 months) and point A7 (AWAC, 1 month). Instrumental data (black points), numerical results (red points). Note the different axes scaling for point A7.

verified in terms of wave period obtained from the resulting maps of Tp that spatially represents the influence of the different wave periods across the numerical domain. Fig. 7 shows the comparison of Tp time series obtained numerically at each of the control points with those of instrumental data. Note the difference in axes scaling of the graph of point A7 with respect to the graphs of points D1 to D6. The time series comparison and their corresponding statistical coefficients show a good general estimation in terms of Tp.

As can be seen in Figs. 6 and 7, the numerical methodology (despite the limitations inherent to linear approaches) is able to adequately solve the dominant processes for wave agitation assessment in the study area. Differences between numerical and instrumental data may be due to additional features not included in the wave modeling, such as locally generated waves, port operations or marine traffic inside the basin influencing the measurements. For the particular case of gauge D1, the deviations may also be due to possible differences of the western numerical contour with respect to the real one, which was unfinished, and under construction, during the field campaign.

In summary, the results obtained for the multiple positions within the port show a general good predictive behavior of this numerical methodology. The historical wave agitation response simulated with this validated downscaling strategy (S1) is considered the baseline below in this work (correlation coefficients in Table 3 demonstrate the best performance). The same catalogue of propagated monochromatic waves used in this validation of S1 has been used for spectral reconstruction of wave agitation response for the preselected cases in all the other hybrid approaches.

4.2. S2: Hybrid, standard theoretical unimodal

This strategy is based on the simplified definition of the outer spectral wave climate by means of the typical set of three aggregated parameters (Hm_0, Tp, Dm). From the 40-year hourly time series, a reduced number of representative sea states (sets of 3 variables) have been selected by using the trivariate MaxDiss selection algorithm (Camus et al., 2011b). According to Camus et al. (2011b), above 200 selected representative sea states, the error in representativeness between each hourly dataset and their representative set stabilizes tending to zero. In the current study, 500 representative cases have been selected from the long time series. Theoretical unimodal spectra (based on Jonswap-TMA spectra, with Wrapped-around Gaussian directional distribution; Massel, 1996) have been used as the forcing spectra for the agitation modeling. Due to the lack of information about frequency and directional spreading in this approach, theoretical/standard values have been assumed ($\gamma = 3.3$ and $\sigma_D = 20°$). In this S2 (as well as in following S3 to S6) hybrid approach, the 500 selected cases are propagated for two different sea levels (low and high water level) to finally obtain the actual results by interpolation for the real sea level. Spectral agitation maps are reconstructed based on the superposition of energy transformed monochromatic waves covering the discretized forcing spectra. From the spectral reconstruction of wave agitation response for the 500 preselected cases, the entire historical series of wave agitation at the target positions have been statistically reconstructed, for each sea level, by means of RBF techniques (Camus et al., 2011a) where the interpolation is based on the 3-parameter hindcast series. The final historical series of wave agitation for the real sea level are obtained by linear interpolation between series for low and high water level.

With this strategy, the common practice for wave agitation prediction of defining the historical outer waves as unimodal sea states from available time series of classical sets of 3 aggregated parameters is assessed.

4.3. S3: Hybrid, characteristic theoretical unimodal

The frequency-directional distribution of wave energy in the outer wave spectra plays an important role in port agitation. When the forcing

spectra for wave agitation modeling are defined by theoretical functions, the wave agitation estimations depends on the spectral shape/spreading coefficients adopted. These parameters vary significantly among different sea states, and theoretical values do not always provide an adequate characterization. This approach is an extended version of the methodology S2 previously described to which the particular/characteristic aggregated parameters of frequency spectral shape (in terms of peak enhancement factor, γ, for Jonswap spectrum) and directional spreading (σ_D) have been added to the set of aggregated parameters defining the sea states in the initial historical time series. Based on Espejo (2011), the γ parameter has been calculated by the expression (Eq. (1)) in the range $1 < \gamma < 7$, where κ (Eq. (2)) is obtained from numerical spectra according to (Rice, 1945); and σ_D has been calculated from directional spectra by using the formula proposed in Kuik et al. (1988) (Eq. (3)).

$$\gamma = \left[\frac{\kappa - 1.869}{-1.465}\right]^{1/-0.1067} \tag{1}$$

$$\kappa(\overline{T})^2 = \left[\frac{1}{m_0}\int_0^\infty S(f)\cos(2\pi(f-\overline{f})\overline{T})df\right]^2 + \left[\frac{1}{m_0}\int_0^\infty S(f)\sin(2\pi(f-\overline{f})\overline{T})df\right]^2 \tag{2}$$

$$\sigma_D{}^2 = 2\left(1 - \sqrt{\left[\left(\int sin\theta\frac{\int S(f,\theta)df}{\int S(f)df}\right)^2 + \left(\int cos\theta\frac{\int S(f,\theta)df}{\int S(f)df}\right)^2\right]}\right) \tag{3}$$

The same methodology of S2 is applied to this S3 based on sets of 5 variables (Hm_0, Tp, Dm, σ_D and γ). The purpose of this version is to quantify the improvement in wave agitation results from a more accurate characterization of outer wave climate considering the actual values of the aggregated γ and σ_D when defining the input spectral information for all the steps of the methodology (selection, definition of the theoretical unimodal spectra, statistical reconstruction).

4.4. S4: Hybrid, combined (unimodal and real-shaped)

A more detailed variation is developed in S4 starting from the same input information as in S2. The same three-parametric time series from S2 is used for S4 for as the initial selection of sea states. That is, the same 500 representative cases selected in S2 are considered here to be numerically transferred to the basin. The difference in this strategy is that the real-shaped spectra (of those 500 preselected sea states) have been used to force the numerical agitation modeling. A rescaling may be necessary in order to exactly match the total energy of the numerically-generated real-shaped spectra with the aggregated H_{m0} values from 3-parametric datasets. The interpolation in the statistical reconstruction (RBF) is based again on the sets of 3 parameters contained in the historical time series.

This alternative is proposed with the idea of obtaining a better estimation of the wave field in the basin since the outer waves considered in forcing the numerical propagations are better (closer to real conditions) represented. Moreover, this version compared to S6 allows to analyze the uncertainty introduced by performing the selection of representative sea states and the subsequent historical reconstruction based on an aggregated parametric definition of waves, disregarding the spectral multimodality of waves.

4.5. S5: Hybrid, characteristic theoretical multimodal

This approach is based on a multimodal theoretical definition (up to three parameterized wave systems) of outer spectra throughout the entire procedure. From the partitioned real shapes of directional spectra, assimilated to typical sea states formed by 2 swells and 1 sea, the historical series composed of 3 hourly sets of 5 wave parameters (3 x {Hm_0, Tp, Dm, σ_D, γ}) has been used as the input information for all the steps in this methodology. Selection of representative sea states has been conducted through an adapted to 15-parameter selection algorithm MaxDiss. Directional spectra used to force the wave agitation estimations have been defined as a superposition of three theoretical sub-spectra (Jonswap-TMA, Wrapped-around Gaussian directional distribution) generated from their corresponding spectral preselected parameters. In this way, a closer approximation to real waves is sought in order to model a more accurate wave agitation response, but without the unfavorable cost of saving the full spectral information, decreasing the size of the input wave database.

4.6. S6: Hybrid, real-shaped

This is the most sophisticated version of hybrid downscaling for wave agitation studies where the whole methodology is based on the real-shaped representation of wave spectra outside the port. The selection of the 500 representative complete spectra is achieved by means of a multivariate statistical downscaling based on the clustering methods described in Camus et al. (2011b), adapted to work with full (frequency-direction) spectra instead of sets of aggregated wave parameters defining the hourly sea states. All the discretized outer spectra comprising the 40-year historical series results in a high multidimensionality of data (N hourly sea states x M frequency-direction pairs (bins) in discretized spectra). Before the application of the selection algorithm MaxDiss, an Empirical Orthogonal Function (EOF) analysis is performed in order to diminish the high dimensionality of data and the excessive computational cost. The original highly dimensional dataset is projected in a new dimensionally-reduced space. The new space is defined by EOFs, as a linear combination of original vectors, in such a way the variation of projected data in that space is maximum (Preisendorfer, 1988). The corresponding hourly temporal amplitudes for EOFs are expressed by Principal Components (PC). The dimensionality is reduced by selecting the P components explaining a certain predefined value of variance, so that $X = \sum_{i=1}^{M} e_i \cdot x_i \approx X' = \sum_{i=1}^{P} EOF_i \cdot PC_i$, where $P < M$. In this case, with a 95% of variance maintained, a reduction of dimensionality of more than one order of magnitude is achieved. The selection and statistical reconstruction techniques are based on these PCs. The 500 preselected sea states are really-shaped represented by their corresponding spectra when forcing the wave agitation modeling.

This hybrid version compared to the dynamic S1 allows to evaluate the uncertainty introduced into wave agitation estimations from hybrid approaches with respect to dynamic propagations. The balance between the quality of results with respect to the computational time involved for both the dynamic and hybrid approaches is quantified (Section 5). Besides, the comparison of this strategy with alternative S4, allows to measure the inaccuracies on wave agitation due to an initial 3-parametric (unimodal) representation of outer wave climate used in selection and statistical reconstruction steps.

4.7. Analysis of forcing spectra definitions and their impact on wave agitation response

The four different approaches adopted to define the forcing spectra in the six proposed strategies for wave agitation modeling are analyzed in this subsection. Spectral shape definitions and corresponding impact on wave agitation predictions are evaluated.

A comparison of different forcing directional spectra generated with each approach for same uni/multimodal sea states is illustrated in Fig. 8. The directional spectra in parameter-based strategies (S2, S3 and S5) have been reconstructed as TMA spectra with Wrapped-around Gaussian directional distributions. In the absence of information, theoretical/assumed values have been considered in S2 for shape and spreading parameters (γ =3.3; $\sigma_D = 20°$). Characteristic values for those historical

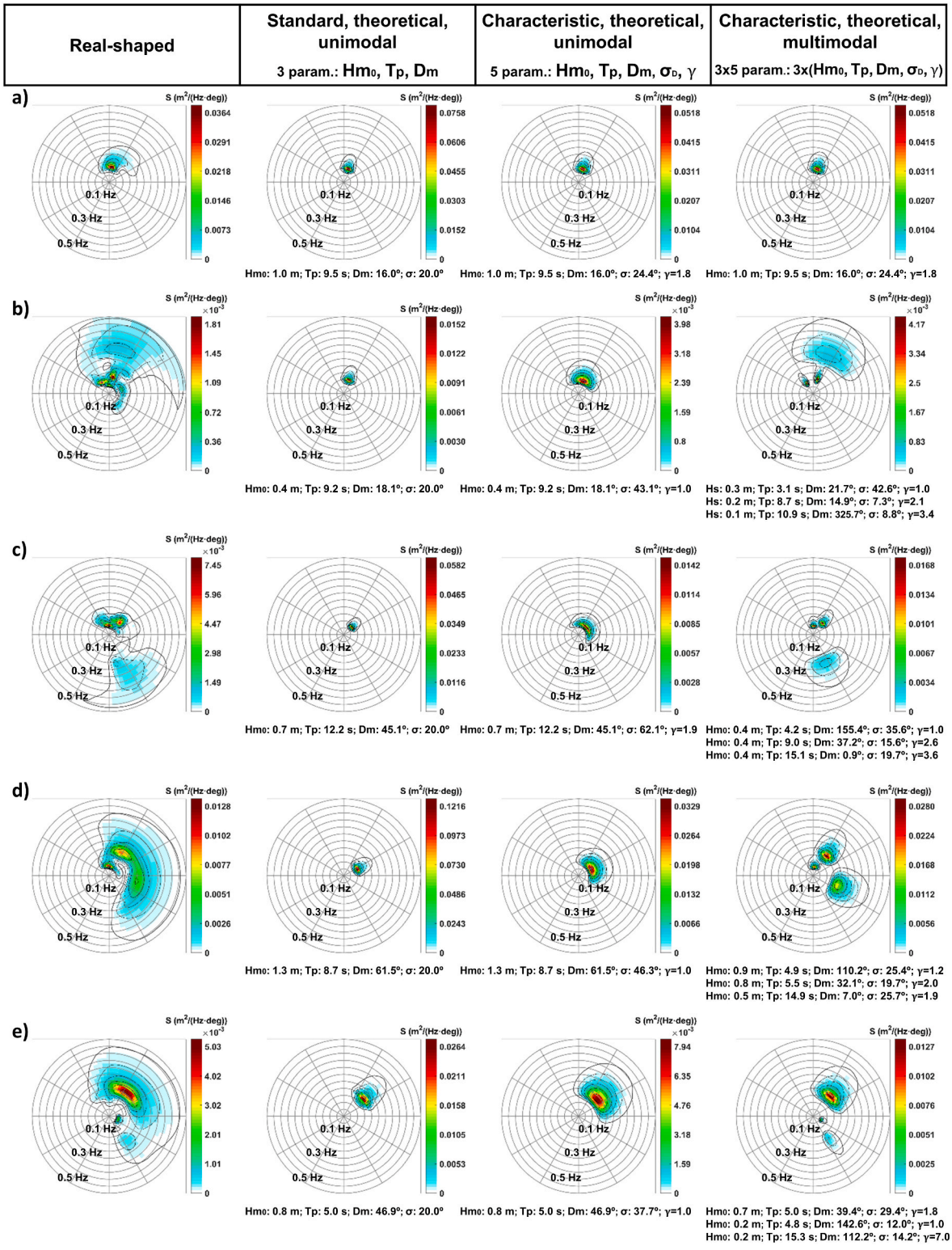

Fig. 8. Sample directional spectra defined as forcing in the wave agitation model for each different approach.

aggregated parameters have been calculated in S3, as well as, those for separate wave systems in partitioned spectra have been determined in S5. Sets of wave parameters used for theoretical reconstructions are indicated in Fig. 8. Strategies S1, S4 and S6 use the complete directional spectra to force the numerical wave agitation modeling. Hm_0, Tp and Tm_{02} values obtained at the 7 control positions by forcing the wave agitation model with the spectra from Fig. 8, are presented in Table 2. The corresponding in-port spectral agitation maps are shown in Fig. 9, where the different wave propagation and agitation patterns are visualized.

For unimodal cases in real-shaped historical time series (case a) in Fig. 8), similar estimations of spectral peaks and general spectral shapes are observed for theoretically-reconstructed spectra, although with narrower distributions both in frequency and direction. Wave energy

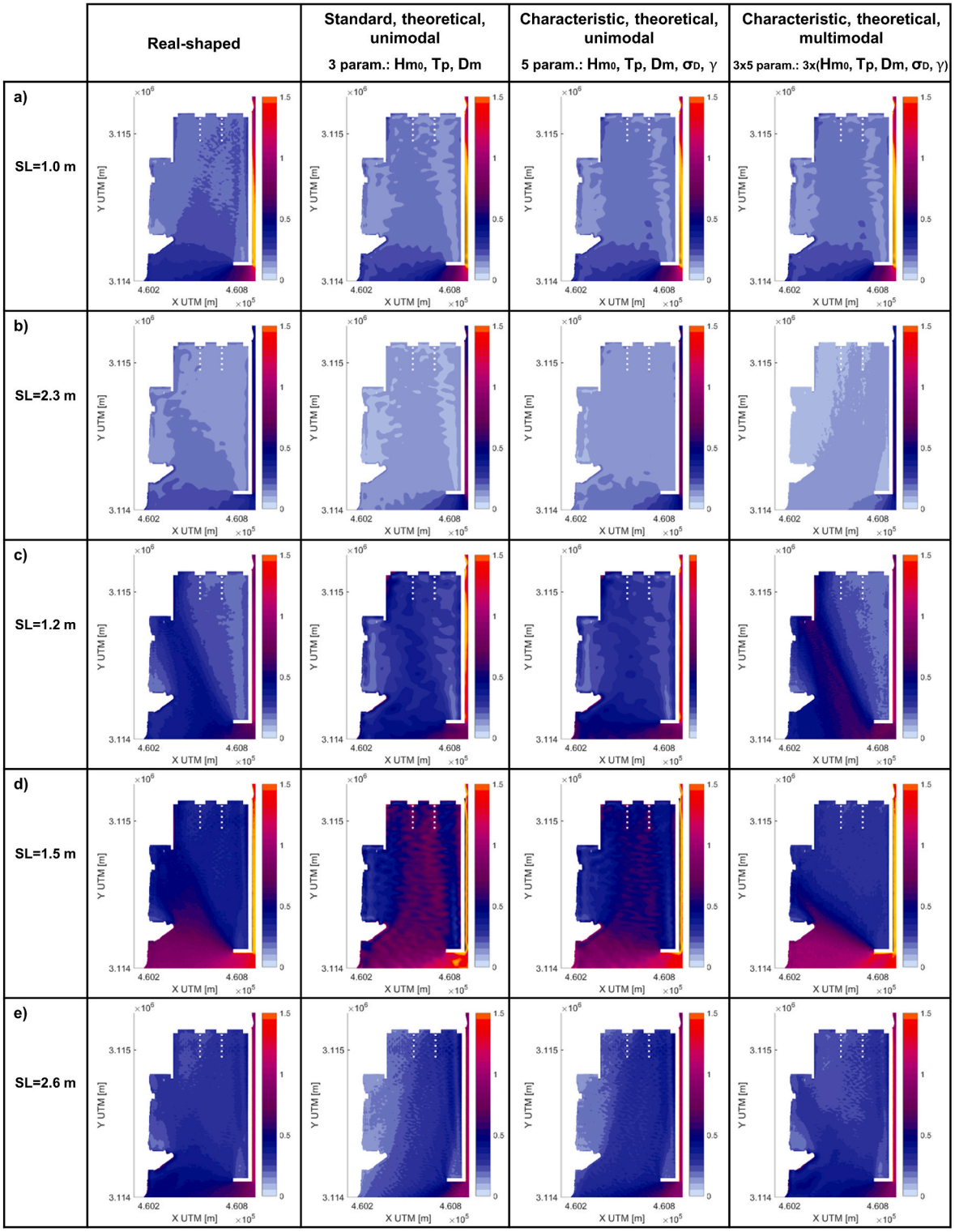

Fig. 9. Spectral agitation maps (Hm_0) obtained for the forcing spectra a) – e) (Fig. 8) in different approaches. SL: Sea Level.

concentrations in more limited frequency-direction ranges are appreciated in directional spectra built from sets of parameters. As can be seen in Fig. 8, the assumed standard values of $\gamma = 3.3$ and $\sigma_D = 20^o$ result in excessively peaked spectra for characteristic outer waves in the study area. Wider theoretical unimodal spectra are reconstructed from characteristic wave parameters. Even so, insufficiently distributed wave energy in the highly influent frequency-direction packages for real agitation (shorter actual periods coming from NE-ENE directions) results in underestimated Hm_0 and higher predicted Tp and Tm_{02} (Table 2). As can be seen in (Fig. 8, case a)), this wave energy exists in real-shaped directional spectrum, while it disappears in directional spectra based on theoretical definitions. Wave energy penetrating towards the eastern side of the port basin is observed in the spectral agitation map from real-shaped forcing spectrum (Fig. 9, case a)), while it does not exist in the other spectral agitation maps from theoretical forcing spectra. This wave energy penetrates towards the eastern area of the basin after reflecting

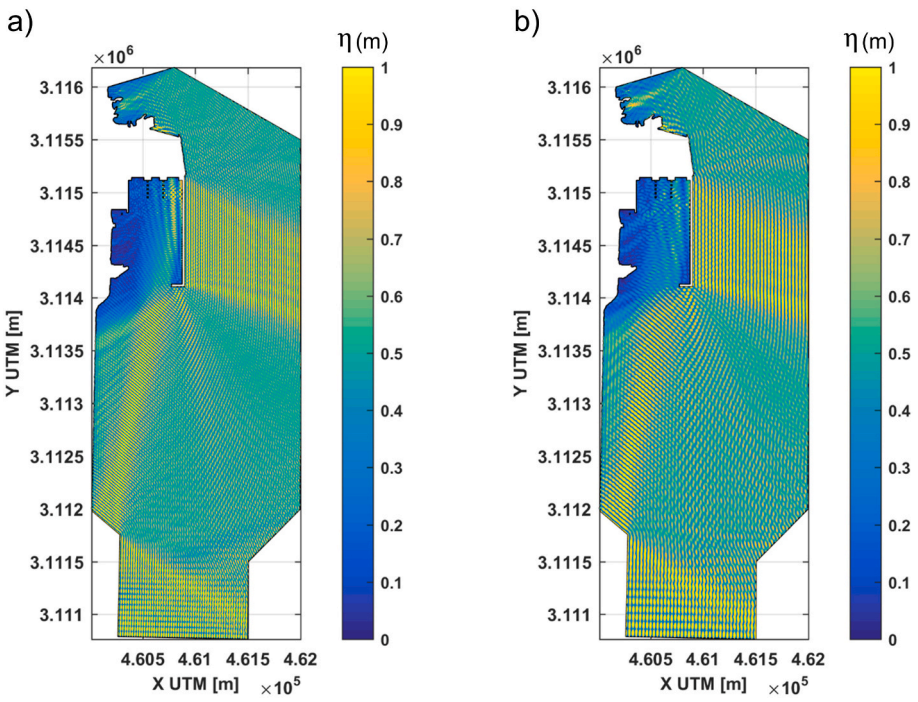

Fig. 10. Normalized free surface maps from propagation with MSPv2.0 model for monochromatic waves with periods of a) 5.1 s and b) 6.2 s, both coming from ENE direction. Visualization of far-field effects on the in-port wave agitation; wave energy penetrating towards the eastern area of the Africa basin after reflecting on the final part of the exterior Reina Sofia breakwater.

on the final part of the exterior Reina Sofia breakwater (about 2.5 km distant from the port entrance). The normalized free surface maps obtained from propagation with MSPv2.0 model for monochromatic waves with periods of 5.1 s and 6.2 s, respectively, coming from ENE direction are shown in Fig. 10. The in-port wave agitation caused by wave reflection from the Reina Sofia breakwater towards the study port basin can be visualized. These far-field effects, caused by the predominant waves (Section 3) in the study area, have an important impact on the wave agitation response of the basin. An accurate characterization of the spectral waves outside the port, in addition to an efficient numerical assembly/strategy for wave propagation over the large port area, are required for an adequate wave agitation characterization in Africa basin.

Noticeable inaccuracies in in-port wave agitation prediction (i.e., significantly shorter periods, Tp and Tm_{02} in Table 2) due to this far-field wave agitation effects, intensified by the narrower theoretical wave energy distribution in triple-peaked spectrum (Fig. 8), are shown in case b). Shorter predicted Tp and Tm_{02} with the characteristic, theoretical, multimodal approach in Table 2, demonstrate the aforementioned (shorter and NE) influent energy components on wave agitation response intensified to the detriment of non-primary longer and northern wave components. Wave energy from SE, directly incident to the basin, is observed in real-shaped agitation map (Fig. 9, case b)). This SE wave energy is not captured by theoretical-based approaches, not even with a trimodal definition, due to the dominance of the more energetic wave components coming from northern directions. Underestimated Hm_0 predictions result from this ignored SE wave energy in forcing spectra in parameter-based approaches (Fig. 8, case b)).

Improved results are obtained from multi-peaked definitions of forcing spectra in clearly multimodal sea states, such as cases c), d) and e) in Fig. 8. In contrast to case b), wave energy coming from SE is represented in theoretical trimodal spectra in cases c), d) and e). Better estimations, closer to real in-port wave field, are clearly shown in Fig. 9 for the trimodal-based approach compared to unimodal ones. Important inaccuracies are observed in wave agitation parameters (Table 2) for both theoretical unimodal approaches. Overestimation is obtained at points D3-D6 because of the wave energy concentration in NE-ENE directions with aggregated spectral definitions, penetrating towards the central/eastern areas of the basin after reflecting on the Reina Sofia breakwater. Additionally, underestimation at point D1 results from unimodal forcing spectra disregarding SE wave systems, even when these are non-primary wave directions, such as case e). Overestimated (in case c)) and underestimated (in cases d) and e)) wave agitation results are obtained for the theoretical trimodal approach, due to narrower energy distributions. Wave component from SE is intensified in the triple-peaked spectrum for case c), resulting in an overestimated wave agitation response in the western area of the basin (points D1 and A7 in Table 2). Conversely, underestimated wave agitation response is obtained from an insufficient wave energy spreading over the most influent energy components in case d).

As a summary, the estimated wave agitation response is clearly determined by the accuracy adopted to define the forcing spectra in wave agitation modeling. Limitations in theoretical spectral shapes result in deviated wave agitation predictions.

5. Results and discussion

The six different strategies presented in the previous section have been applied to the Africa basin (Las Palmas Port). The 40-year time series of wave agitation (Hm_0) at the 7 control points (Fig. 1b) inside the port have been generated by following each methodology (S1–S6). In this section, their performance is evaluated, analyzing the effect of the different approaches adopted for the different steps of the six strategies. The accuracy of each strategy for wave agitation characterization has been measured by comparing the numerical wave agitation results from each downscaling method (S1–S6) with measured data from the field campaign. Grouped data at the 7 control positions are used in comparisons for a clearer interpretation. The main statistical and correlation coefficients obtained for each comparison between data series are summarized in Table 3. In order to quantify the total uncertainty introduced throughout the entire wave downscaling procedure, the initial as well as the accuracy level achieved at previous stage are also presented.

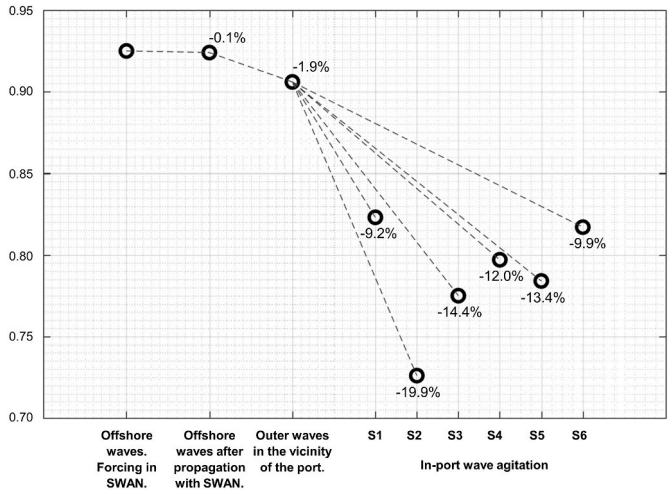

Fig. 11. Correlation coefficient (CORR) of Hm_0 from comparison between numerical and measured data at each step of the wave downscaling procedure. Performance assessment in terms of correlation coefficient reduction (%) from each step to the next one.

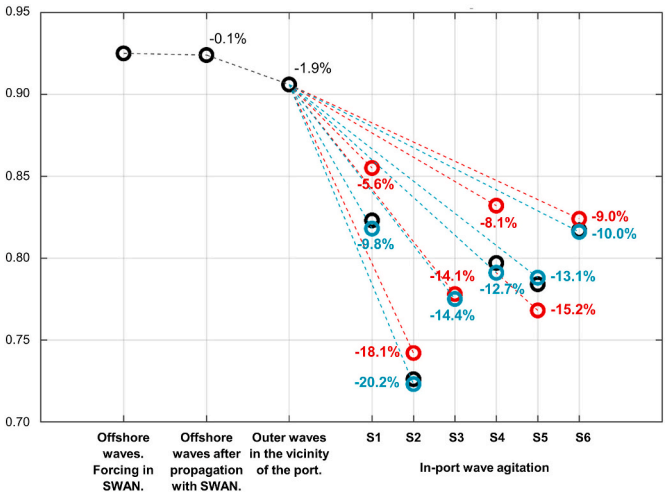

Fig. 12. Correlation coefficient (CORR) from comparison between numerical and measured data at each step of the wave downscaling procedure. Performance assessment in terms of correlation coefficient reduction (%) from each step to the next one. Visualization of global (black) and separated by unimodal (red) and multimodal (blue) sea states correlation analysis for comparison of numerical agitation results with instrumental measurements for each strategy (S1–S6).

Fig. 11 allows the visualization of the uncertainty introduced at each step of the wave downscaling procedure aggregating Table 3 results. The percentage reduction in the bisector correlation coefficient (CORR) from each step to the next one is indicated. Similar behaviour is obtained for the rest of the evaluation coefficients. The high accuracy achieved for wave climate definition outside the port is demonstrated. From high initial correlation values (CORR = 0.92, in terms of Hm_0 at B0 position) for offshore waves, a correlation reduction below 2% is obtained for coastal waves in the vicinity of the port (B1 position), after performing wave transformation modeling with SWAN model in the first stage of wave downscaling. In the second stage of wave downscaling for port wave agitation, the highest correlated predictions are obtained with strategy S1, with an introduced CORR uncertainty of 9.2% with respect to outer/coastal waves. That is, by measuring the total uncertainty introduced from initial offshore waves, with S1, a total correlation reduction of 11% is obtained throughout the entire dynamic downscaling process. In terms of R^2, a total reduction of 20.8% is obtained, while the SI value is 0.24 (Table 3). On the other side, the least accurate wave agitation results are observed for strategy S2, with maximum CORR reductions of 19.9% and 21.5% with respect to coastal and offshore waves, respectively, and SI above 0.42. In summary, the uncertainty in wave agitation prediction is reduced, approximately, by half with the most accurate strategy (the dynamic, real-shaped based S1) compared to the less one (hybrid, standard theoretical unimodal S2). This improvement in wave agitation characterization can be crucial in port operability analyses where downtime is quantified based on H_{m0} operational thresholds. Intermediate levels of accuracy, between those of S1 and S2, are visualized for the rest of strategies (S3–S6). The sequence in descending order of global goodness of fit is the same as increasing the accuracy of outer waves definition: S1, S6, S4, S5, S3, S2.

In Fig. 12, the performance of each strategy (S1–S6) is evaluated separately for unimodal and multimodal (two or more wave components) sea states. The higher accuracy achieved in wave agitation predictions by using more accurate definitions of outer spectra to force the wave agitation modeling is demonstrated not only for multimodal but also for unimodal sea states. As can be seen, poorer estimations are obtained for multimodal (than for unimodal) sea states with all the strategies, except for S5. The slightly lower correlations obtained for unimodal cases with S5 and S6, compared to S3 and S4, respectively, are due to the involvement of null values representing the non-existent wave components in multidimensional interpolation processes, in the final statistical reconstruction step.

As a summary from the analysis of the comparison of the predicted wave agitation values with an 8-month field campaign, good correlation (CORR $\geq$ 0.726, from Table 3 and Fig. 11) is obtained for all the strategies, improving the agitation estimations as the accuracy in defining the forcing spectra increases. Due to the most accurate results presented in Table 3, Figs. 11 and 12, numerical results from strategy S1 are considered as the baseline of the port agitation in the study area. The drawback of this downscaling strategy is the highest computational effort required (Table 4) due to the dynamic approach for wave propagations. In order to evaluate the performance of each hybrid strategy (lower CPU times, Table 4) for practical wave agitation studies based on the complete historical statistics of wave agitation, the 40-year series of numerical results from strategies S2 to S6 have been compared (Fig. 13) with those from the baseline S1.

The aforementioned inaccuracies due to representing the forcing spectra of wave agitation model as single-peaked theoretical spectra are appreciable in results from S2 and S3. Outer multimodal wave energy limited to unimodal distributions results in over/underestimations of wave agitation. Higher goodness of fit is obtained for results for unimodal sea states, although tending to underestimation due to narrower theoretical distributions compared to real-shaped spectra. Slightly improved wave agitation results are observed from S3 (compared to S2) due to a more accurate characterization of outer waves considering the characteristic frequency and directional spreading instead of hypothetical values. The higher availability of historical series formed by sets of aggregated parameters is the main advantage of these methodologies. Another advantage is the low computational effort required (Table 4). However, it is not significantly lower (1.6 h, 3%) than CPU time demanded by S4 or S5 (assuming the required initial information is available), which result in more accurate estimations of historical wave agitation response.

Limitations associated to parameter-based definitions are also observed in S5, which uses trimodal theoretical spectra to force the wave agitation modeling. Deviated wave agitation predictions are obtained due to narrower and more pronounced outer wave energy distributions. Additionally, the reconstructed wave agitation values for unimodal and bimodal sea states are influenced by numerical results obtained for sea states composed of a larger number of wave components. The lack of definition of the wave components are involved in the multidimensional interpolation reconstruction. Overestimated wave agitation results,

Table 4
CPU time involved at each step of the different downscaling strategies for wave agitation studies. CPU times correspond to a PC with characteristics: Intel® Core™ i7-8700 CPU @ 3.20 GHz, 32 GB RAM; except for 40-year propagations with SWAN, executed by using a High Performance Computing Clusters (HPCC).

STRATEGY	S1. DYNAMIC, REAL-SHAPED (baseline)	S2. HYBRID, STANDARD THEORETICAL UNIMODAL	S3. HYBRID, CHARACTERISTIC THEORETICAL UNIMODAL	S4. HYBRID, COMBINED	S5. HYBRID, CHARACTERISTIC THEORETICAL MULTIMODAL	S6. HYBRID, REAL-SHAPED
Historical outer wave climate (Hindcast series)	683.7 h[a]	_[b]	_[b]	_[b] 1.0 h[c]	_[b]	683.7 h[a]
Selection representative cases (MaxDiss, MD)	-	53.0 s	76.5 s	53.0 s	86.9 s	EOF: 248.1 s MD: 540.3 s
Monochromatic waves propagations	2 Sea Levels x 24.1 h[d]	2 Sea Levels x 24.1 h[d]	2 Sea Levels x 24.1 h[d]	2 Sea Levels x 24.1 h[d]	2 Sea Levels x 24.1 h[d]	2 Sea Levels x 24.1 h[d]
Spectral agitation maps reconstruction	371.3 h	2 Sea Levels x 884.2 s	2 Sea Levels x 1 308.9 s	2 Sea Levels x 2003.2 s	2 Sea Levels x 1 319.0 s	2 Sea Levels x 1891.0 s
Historical reconstruction (RBF interpolat.)	-	2 Sea Levels x 99.3 s	2 Sea Levels x 118.0 s	2 Sea Levels x 99.3 s	2 Sea Levels x 242.4 s	2 Sea Levels x 702.2 s
Sea level interpolation	-	3.2 s	3.2 s	3.2 s	3.2 s	3.2 s
Total CPU time	**1 103.2 h**	**48.8 h**	**49.0 h**	**50.4 h**	**49.1 h**	**733.6 h**

[a] CPU time involved in generating the 40-year series of hourly directional spectra in this study, with a High Performance Computing Clusters (HPCC). Execution time for 1-month run: 26.3 h in coarse mesh (22801 nodes); 21.3 h in fine mesh (21901 nodes).
[b] Historical time series of aggregated and partitioned parameters are assumed to be available.
[c] Estimated value as a proportion from total CPU time involved in generating the 40-year series.
[d] CPU time for coarse mesh (design T = 8 s; 107318 nodes; 210637 elements): 16 s/case; CPU time for fine mesh (design T = 5 s; 647599 nodes; 1288347 elements): 204.8 s/case.

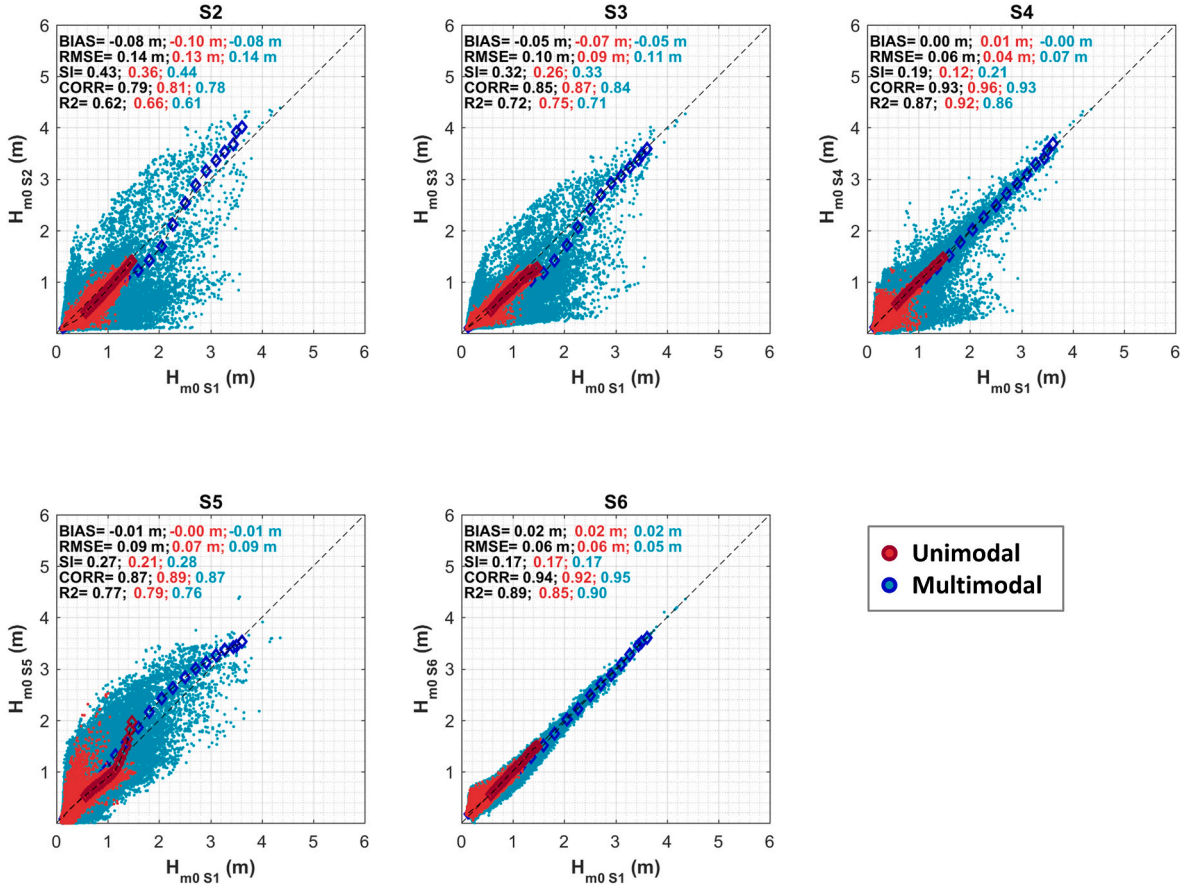

Fig. 13. Comparison (scatter plots and statistical parameters) of each hybrid methodology (S2–S6) versus the baseline (dynamic, S1), separating by unimodal and multimodal sea states. Visualization of global (black) and separated (red: unimodal cases; blue: multimodal cases) goodness of fit. Hm_0 quantile values for 30 non-exceedance probability values equi-spaced between 1% and 99.999%, in Gumbel probability paper, are represented by diamond symbols.

driven by accentuated eastern waves in theoretical multi-peaked forcing spectra (Section 4.7), are observed for both multimodal and unimodal sea states. When historical series of parameterized partitioned wave systems are available, its low computational cost (similar to S2 and S3 in Table 4) while preserving multimodality of waves is an advantage of S5 to be applied in multimodal wave climates for an improved characterization of the wave agitation response.

Higher correlated results with the baseline S1 are achieved for strategies S4 and, mainly, S6. Both are based on real-shaped forcing spectra. Differences between historical results from S4 and S6 demonstrate the influence on wave agitation of different approaches adopted to characterize the outer wave climate at different steps of hybrid methodologies, not only in forcing the wave agitation model but also in selecting the representative sea states and statistical reconstruction. From comparison of goodness of fit for multimodal waves between S4 and S6 (Fig. 12), a relative increment of 27% in CORR uncertainty is introduced in port agitation results due to 3-parametric historical representation of clearly multimodal outer wave climates in selection/interpolation steps. The clear advantage of S4 over S6 and, mainly, over S1 is the high computational time-saving involved (683.2 h, 93.1%; and 1 052.8 h, 95.4%; respectively, Table 4) when the historical time series of outer directional spectra are not available and have to be generated as in the first stage of wave downscaling. Moreover, the CPU time demanded by S4 is almost the same (50 h, approximately; Table 4) as that required by the less accurate parameter-based strategies S2, S3 and S5 (Figs. 11, Figs. 12 and 13). Significantly better wave agitation results are obtained with a little additional computational cost.

The results with the highest correlation, highly close to the baseline S1 (Fig. 13), are achieved with S6, which uses a real-shaped representation of outer spectra throughout the entire hybrid procedure (selection, forcing and reconstruction). These results evidence the high performance of this sophisticated hybrid strategy, with a 33.5% (369.6 h) reduction in CPU time. The slight deviations of S6 with respect to S1 may due to two different factors. On the one hand, due to the uncertainty introduced by a hybrid approach, with respect to a dynamic one, for wave agitation downscaling. On the other hand, due to the percentage of variance neglected in the EOF analysis (5% in this work). It should be noted that CPU effort increases with higher percentages of explained variance.

6. Conclusions

Six different wave downscaling strategies for practical port agitation assessment have been presented in this paper, applied to a study area with a strongly multimodal wave climate in the vicinity of the port (81.6% probability of occurrence), where, in addition, the far-field agitation effects have an important influence on wave agitation inside the basin.

An accurate real-shaped definition of spectral wave climate outside the port has been achieved in a first stage of a dynamic wave downscaling (from offshore to near-port). In a second stage of wave downscaling (from outer waves to wave-in-basin), six different strategies have been developed based on different existing approaches for: a) wave downscaling method and b) definition of multi-annual outer spectral wave climate. The performance/accuracy of each different strategy has been quantitatively evaluated by comparing the numerical results with instrumental data available for an 8-month period. An uncertainty reduction, approximately by half, has been obtained from the most accurate wave agitation results compared to the least ones. This improvement in wave agitation characterization can be crucial in port operability analyses where downtime is quantified based on H_{m0} operational thresholds.

Strategy S1, based on a dynamic real-shaped wave agitation downscaling, has been identified as the baseline for wave agitation characterization in the study area. However, the high computational cost (1 103.2 h) involved in a dynamic propagation of all the outer historical waves into the port results excessive/impossible for practical applications. Therefore, the five hybrid methodologies (S2–S6) have been subsequently evaluated with respect to the baseline in order to evaluate their performance (in terms of accuracy as well as CPU time) for historical wave agitation characterization.

The poorest estimations have been obtained for the parametric approach (S2) based on the simplified definition of the outer spectral wave climate by means of the classical sets of aggregated parameters (Hm_0, Tp, Dm). Single-peaked theoretical spectra are not able to adequately represent the wave energy distribution of multimodal waves when forcing the wave agitation model, resulting in deviated wave agitation patterns. Slightly better results are obtained when considering the characteristic values of aggregated frequency and directional spreading for a 5-parameter (Hm_0, Tp, Dm, σ_D γ) based definition (S3). However, since S3 is based on a unimodal approach, inaccuracies (lower than in S2) due to not representing multimodality of waves are introduced in agitation results. The advantage of these unimodal-based approaches is the greater availability of hindcast database composed of aggregated spectral parameters.

A closer approximation to real-shaped outer spectra has been achieved in S5 by reconstructing the forcing spectra of the wave agitation model as a superposition of up to three theoretical sub-spectra defined from sets of characteristic parameters of spectral partitions (3 x {Hm_0, Tp, Dm, $\sigma_{D,}$ γ}). The advantage of this multimodal theoretical definition is the higher preservation of the multimodal nature of waves (than unimodal definitions) in a more lightly way than containing the complete spectral information. The drawback is (as for parameterizations in S2 and S3) the assumption of theoretical wave energy distributions, producing deviations/concentrations of outer wave energy that result in over- or underestimations of wave agitation.

The high quality results achieved for strategies S4 and S6 demonstrate the importance of forcing the wave agitation model with the real-shaped outer spectra, ultimately resulting in improved wave agitation results. The lower goodness of fit obtained for multimodal sea states with S4, compared to S6, shows the inaccuracies introduced in historical wave agitation estimations due to the simpler 3-parametric representation of outer directional spectra in selection/interpolation steps. S4 is an interesting strategy to be adopted with a reduced number of real-shaped forcing spectra required and the availability of the 3-parametric hindcast. In the absence of available long-term series containing the real-shaped outer spectra, the clear advantage of S4 over S6 is the high CPU time-saving involved (683.2 h, 93.1%). Moreover, the CPU time demanded by S4 is the same (50 h, approximately) as that required by the aforementioned less accurate parameter-based strategies S2, S3 and S5, which makes S4 the most appropriate strategy of these to be followed, if the required initial information is available.

Finally, the most correlated results (with the baseline, S1) achieved for S6 evidence the high performance of this sophisticated hybrid strategy, with the significant computational time-saving involved (reduction of 33.5%, 369.6 h) compared to a dynamic methodology.

To conclude, the reliance of accuracy in wave agitation predictions on the approach adopted to define the forcing spectral wave climate in numerical agitation modeling has been demonstrated. The improvements achieved in characterizing the historical wave agitation response in a harbour by increasing the accuracy in offshore/outer spectral wave climate characterization has been quantified. This can lead to an important uncertainty reduction in harbour design applications. Particularly important could become this analysis in port areas with wave climates greatly affected by effects of climate change, where impacts on in-port wave agitation response can be driven by alterations of outer-harbour wave climate conditions. Furthermore, limitations of the most commonly followed approaches in the last decades for harbour engineering applications, mainly based on unimodal theoretical definitions of waves, have been observed in the comparative analysis. Under/overestimated harbour designs may have resulted, especially in multimodal wave climates, leading to currently existing problems or non-

optimized designs.

In pursuing increased-accuracy port operability/downtime assessments, the uncertainty introduced due to the offshore wave climate definition in wave agitation modeling is reduced in this work. A more accurate (e.g. multidimensional) characterization of in-port wave agitation itself could be the next step to, ultimately, refine the predictions of response of moored ships in harbours, which is the final determining element of the port operability.

CRediT authorship contribution statement

Eva Romano-Moreno: Conceptualization, Methodology, Investigation, Data curation, Resources, Formal analysis, Writing – original draft, preparation. **Gabriel Diaz-Hernandez:** Conceptualization, Methodology, Investigation, Resources, Supervision, Writing - Critical review. **Javier L. Lara:** Investigation, Supervision, Funding acquisition, Writing - Critical review. **Antonio Tomás:** Methodology, Resources, Writing - Critical review. **Francisco F. Jaime:** Investigation, Data curation, Resources, Writing – Critical review.

Declaration of competing interest

The authors declare that they have no known competing financial interests or personal relationships that could have appeared to influence the work reported in this paper.

Acknowledgments

The authors would like to thank the Port Authority of Las Palmas for their cooperation and the information provided; Puertos del Estado (Spanish Ministry of Transport, Mobility and Urban Agenda) for providing the instrumental buoy data.

This work has been supported by a FPU (Formación de Profesorado Universitario) grant from the Spanish Ministry of Science, Innovation and Universities to the first author (FPU18/03046).

This work has been also partially funded under the State R&D Program Oriented to the Challenges of the Society (PID2020-118285RB-I00) of the Spanish Ministry of Science, Innovation and Universities.

References

Booij, N., Ris, R.C., Holthuijsen, L.H., 1999. A third-generation wave model for coastal regions 1. Model description and validation. J. Geophys. Res. Ocean. 104, 7649–7666. https://doi.org/10.1029/98JC02622.

Campos, Á., García-Valdecasas, J.M., Molina, R., Castillo, C., álvarez-Fanjul, E., Staneva, J., 2019. Addressing Long-Term Operational Risk Management in Port Docks under Climate Change Scenarios-A Spanish Case Study, 11. Water, Switzerland. https://doi.org/10.3390/w11102153.

Camus, P., Mendez, F.J., Medina, R., 2011a. A hybrid efficient method to downscale wave climate to coastal areas. Coast. Eng. 58, 851–862. https://doi.org/10.1016/j.coastaleng.2011.05.007.

Camus, P., Mendez, F.J., Medina, R., Cofiño, A.S., 2011b. Analysis of clustering and selection algorithms for the study of multivariate wave climate. Coast. Eng. https://doi.org/10.1016/j.coastaleng.2011.02.003.

Camus, P., Mendez, F.J., Medina, R., Tomas, A., Izaguirre, C., 2013. High resolution downscaled ocean waves (DOW) reanalysis in coastal areas. Coast. Eng. 72, 56–68. https://doi.org/10.1016/j.coastaleng.2012.09.002.

Camus, P., Tomás, A., Díaz-Hernández, G., Rodríguez, B., Izaguirre, C., Losada, I.J., 2019. Probabilistic assessment of port operation downtimes under climate change. Coast. Eng. 147, 12–24. https://doi.org/10.1016/j.coastaleng.2019.01.007.

Cid, A., Castanedo, S., Abascal, A.J., Menéndez, M., Medina, R., 2014. A high resolution hindcast of the meteorological sea level component for Southern Europe: the GOS dataset. Clim. Dynam. 43, 2167–2184. https://doi.org/10.1007/s00382-013-2041-0.

del Estado, Puertos, de Fomento, Ministerio, 1999. Recommendations for maritime works, Series 3, Planning, management and operation in port areas. ROM 3.1-99. Design Maritime Configurat. Ports, Approach Chann. Harbour Basins.

del Estado, Puertos, de Fomento, Ministerio, 2015a. Conjunto de datos. REDEXT.

del Estado, Puertos, de Fomento, Ministerio, 2015b. Conjunto de datos. REDCOS.

Diaz-Hernandez, G., Mendez, F.J., Losada, I.J., Camus, P., Medina, R., 2015. A nearshore long-term infragravity wave analysis for open harbours. Coast. Eng. 97, 78–90. https://doi.org/10.1016/j.coastaleng.2014.12.009.

Diaz-Hernandez, G., Rodríguez Fernández, B., Romano-Moreno, E., L Lara, J., 2021. An improved model for fast and reliable harbour wave agitation assessment. Coast. Eng. 170 https://doi.org/10.1016/j.coastaleng.2021.104011.

Egbert, G.D., Erofeeva, S.Y., 2002. Efficient inverse modeling of barotropic ocean tides. J. Atmos. Ocean. Technol. 19, 183–204. https://doi.org/10.1175/1520-0426(2002)019<0183:EIMOBO>2.0.CO;2.

Egbert, G.D., Bennett, A.F., Foreman, M.G.G., 1994. TOPEX/POSEIDON tides estimated using a global inverse model. J. Geophys. Res. 99 https://doi.org/10.1029/94jc01894.

Eikema, B.J.O., Attema, Y., Talstra, H., Bliek, A.J., De Wit, L., Dusseljee, D.W., 2018. Spectral modeling of wave propagation in coastal areas with a harbor navigation channel. PIANC-World Congr. Panama City 1–15.

Espejo Hermosa, A., 2011. Variabilidad espacial y temporal del recurso surf : metodología y resultados. Tesis Dr. en Red 394.

Gruwez, V., Bolle, a, Verwaest, T., Hassan, W., 2012. Numerical and physical modelling of wave penetration in Oostende harbour during severe storm conditions. In: 5th SCACR Int. Short Conf. Appl. Coast. Res. proceedings, 6th-9th June, 2011 - RWTH Aachen Univ. Ger. Mitteilungen des Lehrstuhls und Instituts für Wasserbau und Wasserwirtschaft der Rheinisch-Westfälischen Tech. H, 165, pp. 198–205.

Hanson, J.L., Tracy, B.A., Tolman, H.L., Scott, R.D., 2009. Pacific hindcast performance of three numerical wave models. J. Atmos. Ocean. Technol. 26, 1614–1633. https://doi.org/10.1175/2009JTECHO650.1.

Kankal, M., Yüksek, Ö., 2012. Artificial neural network approach for assessing harbor tranquility: the case of Trabzon Yacht Harbor, Turkey. Appl. Ocean Res. 38, 23–31. https://doi.org/10.1016/j.apor.2012.05.009.

Kuik, A.J., van Vledder, G.P., Holthuijsen, L.H., 1988. A method for the routine analysis of pitch-and-roll buoy wave data. J. Phys. Oceanogr. 18, 1020–1034. https://doi.org/10.1175/1520-0485(1988)018<1020:amftra>2.0.co;2.

Londhe, S.N., Deo, M.C., 2003. Wave tranquility studies using neural networks. Mar. Struct. 16, 419–436. https://doi.org/10.1016/j.marstruc.2003.09.001.

López, I., López, M., Iglesias, G., 2015. Artificial neural networks applied to port operability assessment. Ocean Eng. 109, 298–308. https://doi.org/10.1016/j.oceaneng.2015.09.016.

Massel, S.R., 1996. Ocean Surface Waves: Their Physics and Prediction. World Scientific, Singapore.

MetOcean Solutions Ltd., 2018. Wavespectra. GitHub – Metocean/wavespectra.

Nortek, 2017. The Comprehensive Manual. Nortek Manuals.

Panigrahi, J.K., Padhy, C.P., Murty, A.S.N., 2015. Inner harbour wave agitation using boussinesq wave model. Int. J. Nav. Archit. Ocean Eng. 7, 70–86. https://doi.org/10.2478/IJNAOE-2015-0006.

Perez, J., Menendez, M., Losada, I.J., 2017. GOW2: a global wave hindcast for coastal applications. Coast. Eng. 124, 1–11. https://doi.org/10.1016/j.coastaleng.2017.03.005.

Preisendorfer, R.W., 1988. Principal Component Analysis in Meteorology and Oceanography. Elsevier.

Rice, S.O., 1945. Mathematical Analysis of Random Noises. Selected Papers on Noise and Stochastic Processes, pp. 132–294. Donver Pub., 1954.

Rueda, A., Hegermiller, C.A., Antolinez, J.A.A., Camus, P., Vitousek, S., Ruggiero, P., Barnard, P.L., Erikson, L.H., Tomás, A., Mendez, F.J., 2017. Multiscale climate emulator of multimodal wave spectra: MUSCLE-spectra. J. Geophys. Res. Ocean. 122, 1400–1415. https://doi.org/10.1002/2016JC011957.

Saha, Suranjana, Coauthors, 2010. The NCEP climate forecast system reanalysis. Bull. Am. Meteorol. Soc. 91, 1015–1057. https://doi.org/10.1175/2010BAMS3001.1.

Saha, Suranjana, Coauthors, 2014. The NCEP climate forecast system version 2. J. Clim. 27, 2185–2208. https://doi.org/10.1175/JCLI-D-12-00823.1.

Thoresen, C.A., 2003. Port Designer's Handbook: Recommendations and Guidelines. Thomas Telford Publishing. https://doi.org/10.1680/pdhrag.32286.

Vílchez, M., Clavero, M., Losada, M.A., 2016. Hydraulic performance of different non-overtopped breakwater types under 2D wave attack. Coast. Eng. 107, 34–52. https://doi.org/10.1016/j.coastaleng.2015.10.002.

Working group PTC II-24, 1995. Criteria for movements of moored ships in harbours: a practical guide (Supplement to bulletin No 88). In: PIANC - Permanent International Association of Navigation Congresses.

Zheng, Z., Ma, X., Ma, Y., Dong, G., 2020. Wave estimation within a port using a fully nonlinear Boussinesq wave model and artificial neural networks. Ocean Eng. 216 https://doi.org/10.1016/j.oceaneng.2020.108073.